

UCSF

UC San Francisco Electronic Theses and Dissertations

Title

Decoding Doublecortin Function Using Cellular Models and Genome Editing

Permalink

<https://escholarship.org/uc/item/55d1492f>

Author

Alvarado, Beatriz Perez

Publication Date

2024

Peer reviewed|Thesis/dissertation

Decoding Doublecortin Function Using Cellular Models and Genome Editing

by
Beatriz Alvarado

DISSERTATION
Submitted in partial satisfaction of the requirements for degree of
DOCTOR OF PHILOSOPHY

in
Developmental and Stem Cell Biology

in the
GRADUATE DIVISION
of the
UNIVERSITY OF CALIFORNIA, SAN FRANCISCO

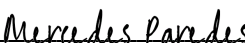
Approved:

DocuSigned by:

77BA96E7DAE34F4... Nadav Ahituv
Chair

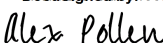
DocuSigned by:

450... John Rubenstein

DocuSigned by:

450... Mercedes Paredes

DocuSigned by:

406... Bjoern Schwer

DocuSigned by:

2102D531BF2D416... Alex Pollen
Committee Members

Copyright 2024

by

Beatriz Alvarado

I dedicate this thesis to my grandmother, Norberta Alvarado, who has served as my most significant source of inspiration for strength, tenacity and wisdom. Despite her lack of any formal education, she always instilled in me the importance of attaining a higher education and nurtured my creativity and passion for knowledge. This accomplishment is for her and all the women who preceded me, who never had the opportunities and privileges that I have been fortunate to receive.

Acknowledgements

Completing this body of work and attaining my Ph.D. has been a protracted and arduous odyssey, marked by challenges and trials. My deepest gratitude to everyone who have played pivotal roles in shaping my academic and personal journey. Their guidance, support, and unwavering belief in my potential have been invaluable throughout this endeavor. I would like to express my sincere appreciation to my mentors, Dr. Bjoern Schwer and Dr. Alex Pollen. Your wisdom, guidance, and dedication to fostering intellectual growth have been instrumental in shaping my research and academic pursuits. Your mentorship has not only enriched my knowledge but has also inspired me to push the boundaries of my capabilities.

A huge thank you to my mother, Irma Alvarado, whose unconditional love and unwavering support have been my anchor through the highs and lows of this journey. Your sacrifices and encouragement have been my driving force, and I am immensely grateful for the values and resilience you have instilled in me. To my grandparents, Norberta and Angel Alvarado, your wisdom and love have been a source of strength. Your stories and experiences have provided me with life lessons that I carry with me every day. Special appreciation goes to my dear friends, Nicole Gallardo and Mimi Namkung, your camaraderie, laughter, understanding and support have been a vital source of balance in my life and to the overall success of my Ph.D. journey. Thank you for standing by me, offering support, and being the pillars of strength that every journey needs.

This acknowledgment would be incomplete without expressing my gratitude to all those who have contributed to my growth, both academically and personally. Your impact on my life is immeasurable, and I am truly fortunate to have such a remarkable support system.

Dr. Dyché Mullins and Dr. Sam Lord provided help and guidance for the live imaging done on transfected fibroblasts. Dr. Bjoern Schwer and Dr. Alex Pollen conceived many of the original ideas for these presented studies and provided valuable insight while supervising this project.

Decoding Doublecortin Function Using Cellular Models and Genome Editing

Beatriz Alvarado

Abstract

Proper establishment of cortical structures during early brain development is vital to normal brain function. A key component of normal lamination of the cerebral cortex is the migration of neurons after they are born from precursor cells to their specific destination in one of the six cortical layers. Neuronal migration involves dynamic changes to microtubules and other cytoskeletal components at the tip of an extending axon or dendrite with the aid of microtubule-associated proteins (MAPs). Doublecortin (DCX) is a MAP that is highly and specifically expressed in immature, migrating neurons. Dysfunction of X-linked DCX causes lissencephaly in males, a malformation characterized by a lack of gyri in the cortex, and subcortical band heterotopia (SBH) or a "double cortex" in females. The role DCX plays in neuronal migration is not well understood and studies in mouse models have only investigated the effects of a complete knockout (KO) of *Dcx*, which resulted in no cortical lamination phenotype in male or female mice, in contrast to the conspicuous phenotypes observed in humans. However, documented disease-causing human DCX mutations involve a missense mutation in one of DCX's microtubule binding domains, which has been shown to not remove DCX function entirely.

Despite characterization of human DCX mutations in patients and mouse Dcx knockout (KO) models, there remains an unmet need for elucidating the cellular and molecular mechanisms of patient-specific mutations in their native genetic context. I hypothesize that the limited phenotypes in Dcx KO mice are due to compensation by other proteins in Dcx's absence, and not due to intrinsic species differences. In particular, I predict that the mutant phenotype observed in the human cortex is due to altered binding to microtubules during neuronal migration, producing a dominant negative effect. To begin to elucidate the role of doublecortin in regulation of neuronal migration, I have introduced a human disease-causing DCX mutation (T203R) into the endogenous mouse Dcx locus. These studies involving the introduction of a disease-causing, patient-derived mutation into the endogenous Dcx locus in the mouse genome have yielded important insights into the biology of doublecortin and cortical development, addressing unresolved mechanisms of patient-specific DCX mutations at the molecular and cellular level.

Table of Contents

CHAPTER 1: INTRODUCTION	1
1.1 Cortical development and Neuronal Migration	2
1.2 Microtubule Associated Proteins and Doublecortin	4
1.3 DCX Phosphorylation and Protein Interactions	6
1.4 Doublecortin Mutations and Phenotypes	7
1.5 Impact of Dcx mutations on MT colocalization and morphology	9
1.6 Impact of DCX mutations on neuronal migration	12
1.7 Aggregate formation	14
1.8 Dcx-T203R Mutation	15
1.9 Summary	16
CHAPTER 2: MATERIALS AND METHODS.....	17
CHAPTER 3: RESULTS.....	25
3.1 Dcx-T203R introduction <i>via</i> Gene Targeting	26
3.2 Targeted mESC Neuronal Differentiation	37
3.3 Dcx T203R MT binding dynamics	53
3.4 Dcx-Microtubule Binding Dynamics vs. Dcx-T203R Competitive Binding Along Microtubules	58
CHAPTER 4: DISCUSSION.....	64
CHAPTER 5: REFERENCES.....	71

List of Figures

Figure 1.1 Doublecortin Protein Structure and binding	11
Figure 3.1 Experimental Overview	28
Figure 3.2 DCX T203R Expression Upon Transient Transfection	29
Figure 3.3 Introduction of Dcx-T203R Mutation at Endogenous Locus	32
Figure 3.4 Validation of T203R Knock-in mouse ESCs	35
Figure 2.5 Sequencing of Dcx cDNA Transcript	36
Figure 3.6 Neuronal Differentiation Protocol Schematic	39
Figure 3.7 Cell Type Composition of Differentiation Culture	42
Figure 3.8 Neuronal Differentiation Quantification of Regional Marker Foxg1.....	45
Figure 3.9 Derived Neurons Immunofluorescence	48
Figure 3.10 Spn and Dcx Aggregates in Derived Neurons	49
Figure 3.11: Neuronal Migration Assay	52
Figure 3.12 Dcx binding Intensity in Transfected Fibroblasts	55
Figure 3.13 Dcx and EB1 Localization in Transfected Fibroblasts	57
Figure 3.14 Dcx-T203R shows low affinity for microtubules.....	60
Figure 3.15 Subcellular Fractionation	63

List of Abbreviations

Intermediate progenitor cell (IPC)

Cortical plate (CP)

Microtubules (MTs)

Immunofluorescence (IF)

Microtubule-associated proteins (MAPs)

Doublecortin (DCX)

Doublecortin-like kinase 1 (DCLK1)

Serine/threonine (S/T)

Spinophilin (SPN)

Filamentous actin (F-ACT)

Subcortical band heterotopia (SBH)

Knockout (KO)

Doublecortin-like kinase 1 (DCLK1)

RNA interference (RNAi)

Induced Pluripotent Stem Cells (iPSCs)

Mouse embryonic stem cells (mESCs)

Clustered Regularly Interspaced Short Palindromic Repeats (CRISPR)

Long-range polymerase chain reaction (LR-PCR)

Complementary DNA (cDNA)

Chapter 1: Introduction

Cortical development and Neuronal Migration

The recent expansion of the human cerebral cortex is thought to underlie our enhanced cognitive abilities (Geschwind & Rakic, 2013). The cortex is a highly complex and organized structure that requires an intricate and precise developmental process in order to be established properly (Cadwell et al., 2019). The expansion of the cortex is a consequence of the increased proliferative capacity of different neural progenitor cell types that is seen in humans as opposed what has been observed in non-human primates and mice (Lui et al., 2011). Our increased cognitive abilities rely on the precisely orchestrated migration of neurons from the cortex's ventricular zone into established neuronal layers. The organization of the cortex consists of columns positioned radially to the cortical surface, established by proliferative units in the germinal zones (GZs). Excitatory projection neurons and inhibitory interneurons are the basic neuronal components that comprise the cortex. Excitatory neurons originate from the dorsal ventricular zones migrating radially into cortical columns, while inhibitory neurons originate from ganglionic eminences of the basal forebrain, migrating tangentially to the cortex (Lim et al., 2018), with some recent reports of cortical-born inhibitory neurons in humans (Delgado et al., 2022).

Neurogenesis begins at approximately embryonic day (E)33 in the human dorsal telencephalon and E10 in mice (Clancy et al., 2001; Stepien et al., 2020). This period in cortical development follows a series of proliferative symmetrical divisions and asymmetrical divisions of radial glial cells in the periventricular neuroepithelium (Kriegstein et al., 2006). Asymmetric radial glia cell divisions produce one daughter cell that will remain a radial glia cell and one post-mitotic cell that will either give rise to a

neuron or a glial cell. Neurons can be produced either directly from radial glia or indirectly through an intermediate progenitor cell (IPC). The pool of IPCs further contributes to the formation of the subventricular zone and undergoes transit amplification in humans increasing the neuronal output of individual radial glia (Martinez-Cerdeno, 2006; Noctor et al., 2004). Neurons then migrate to their destination in the cortical plate (CP) along the processes of progenitor cells (Noctor et al., 2004).

The adult neocortex is organized in six radial layers (I-VI). The neocortex develops in an “inside-out” manner, with deep layers established first and the upper layers established after. Proper layering is critical for functional synapse formation throughout the cortex and perturbations in this process can lead to severe brain malformations, epilepsy, and cognitive deficits (Moffat et al., 2015). Proper layering by normal neuronal migration is also essential for cortical function that a proper ratio of inhibitory neurons migrate to the cortical plate from CGE and MGE and establish correct localization among excitatory neurons in their corresponding layers of the cortex.

To achieve the proper architecture of the cerebral cortex in which neurons are precisely organized and differentiated into distinct and specific layers, accurate neuronal migration to the neuron’s specific destination is required. Neuronal migration is an intricate cellular process that requires complex and dynamic reorganization of their cytoskeletal structure. Microtubules (MTs) and actin filaments are some of the cytoskeletal components that are key to neuronal movement. MTs are composed of protofilament strands made up of alpha and beta tubulin heterodimers that string together to form hollow cylinders. In the human cortex, 13-protofilament strands are preferentially nucleated and assembled (Moores et al., 2004). Microtubules play many

critical roles in cellular functions such as intracellular transport, cellular migration and cell division through the process of regulated MT polymerization and MT shortening by depolymerization (Dema et al., 2024; Ettinger et al., 2016).

Microtubule-associated Proteins and Doublecortin

Cytoskeletal restructuring employs a subset of proteins that are designated to help with this reorganization. Microtubule-associated proteins (MAPs) are a class of multiple proteins that interact with microtubules and tubulin monomers to help regulate their structure and changes that occur. MTs are in constant dynamic instability that require the interaction with various different components, and MAPs serve as an interface for them. There are many different proteins that have been classified as MAPs and these include MT stabilizers, destabilizers, capping proteins and motor proteins (Rice, 2001; Vallee et al., 2004; Zheng et al., 1995).

The category of Doublecortin (DCX) proteins, which serve to stabilize microtubules (MTs), possess distinct MT-binding domains known as doublecortin (DC) domains, setting them apart from other microtubule-associated proteins (MAPs) (Fig. 1A) (Reiner et al., 2006). This family, comprising eleven paralogs in both human and mouse, exhibits specialization and divergence in its N-terminal and C-terminal domains (Reiner et al., 2006). The gene DCX was initially identified in 1998 in an analysis studying the brain cortical malformations of the patients (Gleeson et al., 1998). DCX is found specifically in immature neurons, and is 40 kDa in length. Dcx has been shown to be essential for neuronal migration in embryonic and postnatal brain development. Patients that have mutations in the DCX-encoding gene exhibit lissencephaly in males

and subcortical band heterotopia (SBH) in females (Gleeson et al., 1998). This type of human developmental diseases are the result of perturbations to neuronal migration of cortical neurons which lead to severe mental retardation and seizures among other complications. Notably, certain members of the DCX family, like DCX and Doublecortin-like kinase 1 (DCLK1), exhibit high expression levels in various cancer cells (Ye et al., 2023).

However, the exact mechanism underlying DCX's involvement in cell migration remains unclear, though it is believed to be linked to its influence on MT structure, particularly thickness and stability, as well as the regulation of MT-actin interactions. Structurally, DCX comprises tandem doublecortin-like (DC) domains, including an N-terminal (N-DC) and a C-terminal doublecortin-like domain (C-DC), crucial for MT binding, with both domains sharing 27% sequence identity (Fig. 1A) (Moslehi et al., 2017). It is important to note that both DC domains and the linker region are necessary for achieving a stabilization of MTs (Rafiei et al., 2022). Both DC domains and the linker region are essential for MT stabilization, while the C-tail region facilitates specific binding to 13-protofilament MTs, characteristic of neuronal MTs *in vivo* (Bechstedt & Brouhard, 2012). Specifically, DCX binds to the fenestrations between α and β tubulin monomers, at the junction of the four α/β -tubulin dimers along the length of MT filaments with the exception of the MT plus ends (Ettinger et al., 2016)(Moore et al., 2004). Experimental evidence indicates that only constructs containing both DC-binding domains effectively associate with MTs, emphasizing the necessity of both domains for MT co-assembly (Taylor et al., 2000). Moreover, the C-DC domain of DCX binds to both assembled microtubules and unpolymerized tubulin monomers (Kim et al., 2003). DCX

can also self-associate via its C-DC and C-tail domains, forming an extended structure that acts as a lateral and longitudinal scaffold, thereby enhancing MT stability and interactions with other MTs and actin filaments (Rafiei et al., 2022).

The two DC binding domains within DCX consist of an N-terminal repeated domain and a C-terminal serine/proline rich domain, which contain multiple phosphorylation sites for serine/threonine (S/T) kinases such as c-Jun N-terminal kinase (JNK) and cyclin-dependent kinase 5 (Cdk5) (Gleeson et al., 1999).

DCX Phosphorylation and Protein Interactions

DCX phosphorylation plays an important role in the interactions between DCX and either MTs or actin filaments (Bott et al., 2020; Tanaka et al., 2004). Phosphorylation of DCX has been shown to alter its affinity for MTs and can regulate neurite extension as well as neuronal migration (Reiner et al., 2004; Schaar et al., 2004; Tanaka et al., 2004). Cdk5, is one of many S/T kinases that are primarily active in terminally differentiated neurons (Ohshima et al., 1996). Cdk5 phosphorylation of DCX at serine 297 within the DCX C-DC reduces its affinity for MTs and its ability to polymerize tubulin (Tanaka et al., 2004). Studies looking at S297 phosphorylation showed that DCX mutants lacking S297 phosphorylation site led to neuronal migration defect (Tanaka et al., 2004). Another study showed that JNK phosphorylation of DCX at S332 in vivo is critical for the regulation of DCX binding to tubulin (J. Jin et al., 2010). The dynamic nature of cytoskeletal reorganization which underlies neurite outgrowth and migration, predicts that DCX phosphorylation, like that of many other MAPs, is highly regulated by both kinases and phosphatases. Mutations which interfere with

phosphorylation or dephosphorylation of DCX may therefore perturb its binding along MTs or actin filaments.

DCX interactions with actin filaments are facilitated through interactions with Neurabin II/ Spinophilin (SPN) (Tsukada et al., 2003). SPN has an N-terminal coiled-coiled domain that binds to a portion of the DCX C-DC domain and the N-terminal portion of the Ser/Pro-rich domain, as well as binding sites for F-Actin (F-ACT) (Tsukada et al., 2005). An SPN-DCX heterodimer has been shown to be involved in neuronal migration by mitigating MT bundling at the wrist region during neurite extension (Tsukada et al., 2005). The actin-associated SPN located at the neurite wrist enhances the dephosphorylation of DCX, which reinstates DCX's microtubule-associated activities. This then allows the orderly bundling of MTs into the neurite shaft, thus propelling the axon growth cone and assisting in neuronal migration (Bielas et al., 2007; Tsukada et al., 2003). The interaction between SPN and DCX promotes the transfer of DCX from microtubules to filamentous actin (F-ACT) and orchestrates the functions of microtubules and F-ACT in neuronal cells. These processes play a crucial role in cortical maturation and brain development.

***Doublecortin* Mutations and Phenotypes**

Mutations in *DCX* have been shown to lead to distinct morphological changes in cortical structure. The phenotypes associated with *DCX* mutations vary between male and female, due to *DCX* being an X-linked gene. Male patients with *DCX* mutations develop lissencephaly, a complete smoothing of the cortex, while female patients have double-cortex syndrome or subcortical band heterotopia (SBH), where there is a

band of gray matter embedded in the white matter of the cortex (Gleeson et al., 1998). An analysis of human patients with SBH revealed that 100% of cases are due to mutations in *DCX*.

However, previous studies investigating *Dcx* function using mouse models have only studied it in the context of a complete knockout (KO) of *Dcx* (Chang et al., 2018; Dhaliwal et al., 2015; K. Jin et al., 2010; Kerjan et al., 2009). These germline *Dcx* knockout mice do not recapitulate the human cortical phenotypes of SBH and lissencephaly, but do display aspects of hippocampal disorganization and agenesis of the *corpus callosum* that mirror patient phenotypes (Chang et al., 2018; Dhaliwal et al., 2015; Nosten-Bertrand et al., 2008). It is not known if these dramatic differences in cortical phenotypes are due to the different approaches used (*i.e.*, complete ablation of *Dcx* in mouse models vs. *DCX* point mutations in humans) or if they are due to species-specific differences in cortical development. Notably, disease-causing *DCX* mutations in humans involve missense mutations in either of the doublecortin protein domains, rather than complete loss of the *DCX* protein. The two doublecortin protein domains are responsible for the tubulin binding properties of *DCX*, suggesting that human disease-causing mutations are altering *DCX*'s binding properties and could be acting as a dominant negative (Manka and Moores 2020; Rafiei et al. 2022; Ayanlaja et al. 2017; Reiner et al. 2006).

In contrast, complete loss of *DCX* may permit compensatory mechanisms to take place. For example, doublecortin-like kinase 1 (DCLK1) and doublecortin-like kinase 2 (DCLK2) also have two doublecortin binding domains and may bind both α and β tubulin in the complete absence of *DCX*, whereas *DCX* with only one functional doublecortin

domain cannot bind to polymerized tubulin. This may explain the lack of a cortical phenotype in mice, and potentially offer avenues for intervention in patients with missense mutations. However, as outlined above, the impact of missense mutations of endogenous *Dcx* on cortical development has not been investigated in mice.

The influence of DCX mutations on microtubule binding, aggregate formation, morphology, cell fate potential, and neuronal migration have been shown (Dema et al., 2024; Deuel et al., 2006; Moores et al., 2004; Yap et al., 2016). Despite important mechanistic findings from cellular models, most studies involve ectopic overexpression or complete loss-of-function, and many patient-specific mutations have not yet been analyzed. The following section reviews recent mechanistic studies in cell-based models and complementary evidence from mouse models.

Impact of *Dcx* mutations on MT colocalization and morphology

In migrating neurons, *Dcx* colocalizes with 13-protofilament MTs through interactions with both DC-domains. Specifically, it binds within the fenestrations of the alpha and beta tubulin monomers that make up MTs (Fig. 1C) (Francis et al., 1999; Gleeson et al., 1999). The two binding domains are repetitive elements that are predicted to have the secondary structure of a β -grasp superfold motif (Fig. 1B) (Taylor et al., 2000). The importance of these interactions is demonstrated in that lissencephaly- and SBH-causing mutations cluster along the two DC-domains (Fig. 1B). Mutations found within the two repetitive DC-domains alter binding along the cytoskeleton as well as *Dcx*'s ability to nucleate, polymerize and stabilize MTs (Kim et al., 2003; Moores et al., 2004; Yoshiura et al., 2000). Previous studies that have

modeled *Dcx* mutation in mouse cells have shown that mutant *Dcx* does colocalize to MTs, except for some particular mutants, such as the two mutants at position 125: Y125D and Y125H, which fail to colocalize at all (Yoshiura et al., 2000). Although colocalization with MTs occurs, mutant *Dcx* has been shown to be expressed at far lower levels than WT (Shahsavani et al., 2018; Yoshiura et al., 2000). There are also notable changes to the morphology of *Dcx* mutant cells. Complete ablation of *Dcx* results in excessively branched axonal shafts in the migrating neurons of mice (Kappeler et al., 2006; Koizumi et al., 2006). Additionally, *Dcx* KO does not result in any other morphological changes such as alterations in dendritic complexity, number of branches, and total dendritic length (Merz & Lie, 2013). However, *Dcx* mutations have been shown to cause a reduction in overall dendritic complexity and enhanced dendrite growth as was also seen with *Dcx* overexpression (Cohen et al., 2008; Yap et al., 2016).

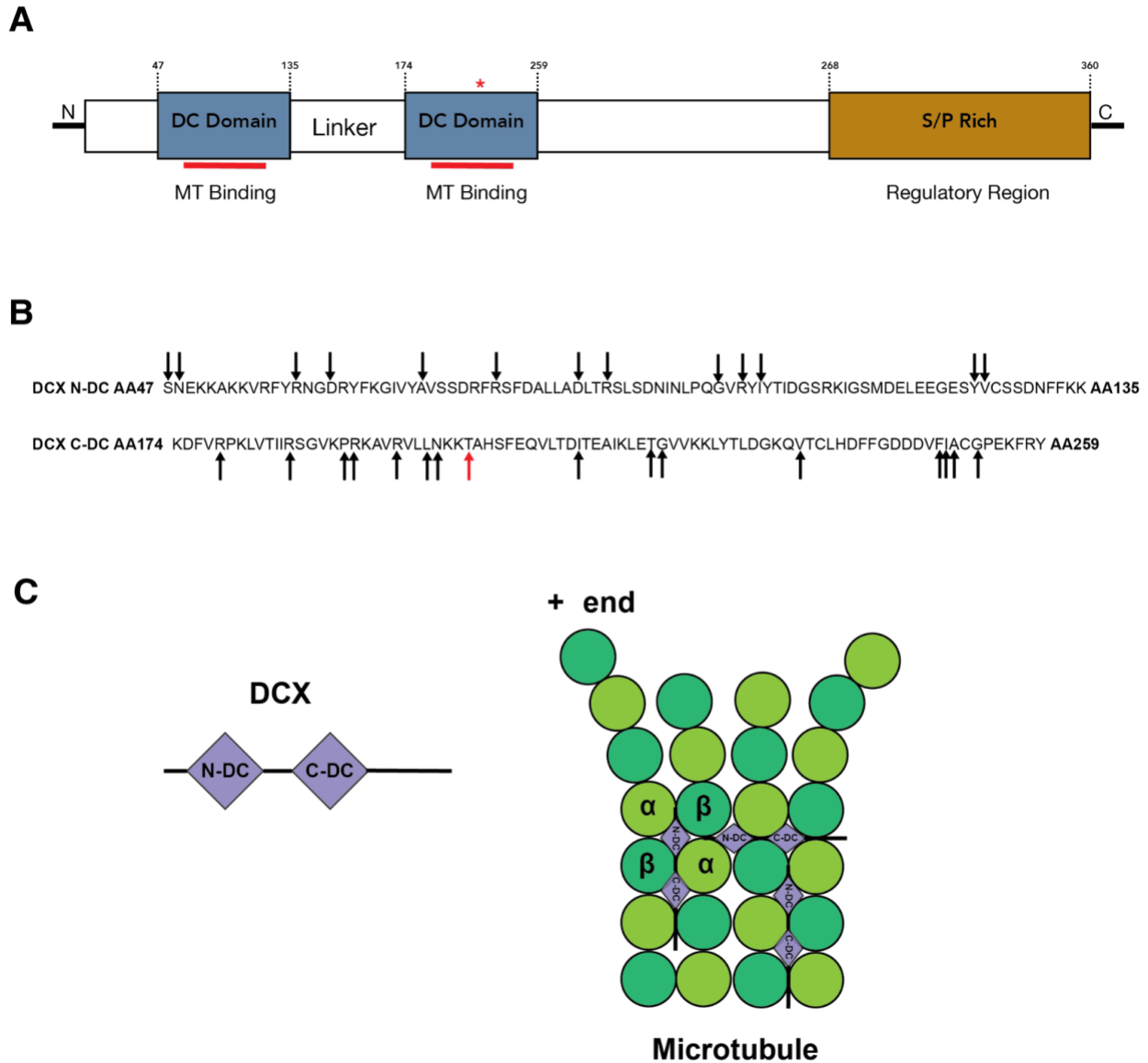


Figure 1.1: Doublecortin Protein Structure and binding

(A) Dcx protein schematic highlighting both MT binding DC-domains (red lines) and the location of the Dcx-T203R mutation in the C-terminal DC-domain. The schematic also shows the serine/proline rich domain (tan) which is a regulatory region for the protein. **(B)** The amino acid sequence of both Dcx DC-domains, showing similarity of both domains, known human mutations (black arrows) and Dcx-T203R mutation highlighted (red asterix) **(C)** Schematic representation of Dcx protein structure and binding along MTs. (Left) Illustration of Dcx protein structure, (Right) Dcx binding to fenestration of tubulin monomers along MTs. Adapted from (Moore et al., 2004; Rafiei et al., 2022).

Impact of DCX mutations on neuronal migration

To migrate during cortical development, neurons extend a process radially along radial glia scaffolds through the development of axon growth cones (Accogli et al., 2020; Dun et al., 2012; Nowakowski et al., 2016). *Dcx* KO studies in mice have revealed no cortical migration phenotypes but they did show decreased migration velocity and delamination of the hippocampus in the CA3 region (Chang et al., 2018; Corbo et al., 2002; Pramparo et al., 2010). Notably, there is a significant difference in migration phenotype seen in rats after RNA interference (RNAi)-mediated knockdown of *Dcx*. Utilizing *in-utero* electroporation, one study found that RNAi of *Dcx* in rat cortex disrupted the cell-autonomous and non-cell autonomous radial migration of neurons. In the rat cortex, knockdown of *Dcx* by RNAi recreated the SBH phenotype seen in humans and also showed altered lamination of the cortex (Bai et al., 2003; Ramos et al., 2006). However, when these experiments were replicated in mice, the RNAi did not lead to SBH but did disrupt the neocortical lamina (Ramos et al., 2006). These results suggest, at least in part, that *Dcx* KO may trigger compensatory responses from other MAPs that prevent the onset of phenotypes resembling the phenotypes observed in human patients with *DCX* mutations, which do not occur upon acute, RNAi-mediated *Dcx* knockdown.

Indeed, *Dcx* has homologs in mice that can act to compensate for its complete ablation. Doublecortin-like kinase 1 (*Dclk1*) and doublecortin-like kinase 2 (*Dclk2*) both contain DC-domains and can bind MTs. Both *Dclk1* and *Dclk2* have broad expression throughout the nervous system, including mitotic neuroblasts and adult neurons, whereas *Dcx* is mostly expressed in postmitotic immature neurons. In mice, KO of either

Dcx or *Dclk1* does not lead to migratory defects in the cortex, but a *Dcx/Dclk1* double KO does cause abnormal cortical architecture (Deuel et al., 2006). In contrast, *Dcx/Dclk2* double KO mice do not show altered cortical structure but do show delamination of the hippocampus at regions CA1 and CA3, similar to what is seen with *Dcx* KO mice (Kerjan et al., 2009).

In-vivo studies have used KO and RNAi knockdown of *Dcx* to analyze phenotypes but have not tested any of the human disease-causing patient mutations. Some of these mutations have been investigated *in vitro* by overexpression of mutant *Dcx* in cells with or without endogenous *Dcx* expression. Two *DCX* mutations that have been analyzed *in vitro* by generating human patient-specific iPSCs, and then differentiating neurons (Shahsavani et al., 2018). However, that study did not include any missense mutations along the C-terminal DC domain. Shahsavani *et al.* reported that mutations in the C-terminal DC domain of *DCX* show more severe phenotypes than those occurring in the N-terminal DC domain. Mutations in the C-terminal DC domain caused slower migration velocity and an overall decrease in total neuronal migration (Shahsavani et al., 2018; Yap et al., 2016). Furthermore, mutations in either DC domain caused a decrease in dendrite complexity and thickness (Shahsavani et al., 2018; Yap et al., 2016). Even though there has been an increase in the study of *Dcx* nonsense and missense mutations, the molecular and cellular defects for most of them are still only incompletely understood and most have not been investigated at the level of endogenous expression.

Aggregate formation

Some of the studies that have investigated human disease-causing mutations *in vitro* have observed that certain *Dcx* mutants cause the formation of protein aggregates in the cytoplasm of cells (Sapir et al., 2000; Yap et al., 2016, 2018). This phenotype has not been thoroughly characterized but is of great importance, as protein aggregates drive many neurodevelopmental disorders and may play an important role in the severity of the cortical malformations caused by the mutation.

Previous studies used an *ex-vivo* overexpression approach in order to introduce a number of DCX disease causing patient mutations into dissociated rat cortical neurons from E18 embryos (Yap et al., 2016, 2018). Specifically, rat hippocampal neurons were electroporated with plasmids expressing the mutant DCX (Yap et al., 2016). Overexpression of mouse *Dcx*-R59H caused detergent-insoluble aggregates in the cytoplasm that colocalized with both SPN and ubiquitin (Yap et al., 2016). The colocalization of DCX with SPN is particularly intriguing because their association plays a vital role in DCX's movement into the axon growth cone.

The phosphorylation of DCX is implicated in mediating interactions between MTs and F-ACT, which is crucial for neurite outgrowth, formation of axon growth cones and neuronal migration (Tanaka et al., 2004; Tsukada et al., 2003, 2005). SPN forms a complex with phosphorylated DCX and is shuttled from MTs in the axon wrist of neurons into the F-ACT structures inside the axon growth cones (Bott et al., 2020; Tsukada et al., 2006). Through this mechanism, the SPN-DCX interaction plays a key role in neuronal migration and dendritic spine formation. Thus, certain DCX mutations may disrupt the interaction with SPN and cause morphological and migratory

phenotypes (Bielas et al., 2007; Bott et al., 2020; Rafiei et al., 2022). There are several kinases active in neurons that phosphorylate DCX at serine 297, reducing its affinity for MTs and overall tubulin polymerization (J. Jin et al., 2010; Schaar et al., 2004; Tanaka et al., 2004). SPN has also been shown to enhance protein phosphatase 1 (PP1)-mediated dephosphorylation of DCX at key residues, (Shmueli et al., 2006; Tsukada et al., 2003, 2006). The dynamic regulation of DCX phosphorylation, involving both kinases and phosphatases, is crucial for cytoskeletal reorganization during neurite outgrowth, axon growth cone formation, and neuronal migration. More work is needed to define the mechanism by which DCX mutations affect its phosphorylation and may cause its aggregation.

Dcx-T203R Mutation

There are many DCX mutations that have been identified in patients with subcortical band heterotopia (SBH), a majority which reside in either DC domain of DCX. DCX-T203R is a missense mutation in the C-terminal doublecortin binding domain that has been shown to have a notable phenotype (Matsumoto et al., 2001; Taylor et al., 2000). The DCX-T203R mutation is both familial and sporadic and has not been studied in detail (Gleeson et al., 1999). I have selected this mutation because of its dramatic decrease in MT polymerization in vitro, even when compared to other DCX patient mutations (Taylor et al., 2000).

Summary

Previous work done to elucidate DCX's function during cortical development have utilized multiple methods to assess the phenotypes seen in human patients with *DCX* mutations. *In vivo*, *Dcx* KO mice have failed to recapitulate the cortical migratory phenotype seen in patients. *In-vitro* studies have used overexpression of human disease-causing *DCX* mutations in cells that do not endogenously express *DCX* and have shown cellular and morphological phenotypes. However, overexpression experiments make disentangling phenotypes resulting from the mutation versus those that result from over-expression very difficult. This thesis work uses gene editing to knock-in a specific *DCX* mutant (*DCX-T203R*) in order to closely investigate the effect that the mutation has on *DCX* function which can yield fundamental insights into the resulting phenotypes seen in humans. This introduction of a disease-causing human patient mutation into the mouse endogenous locus has not been done previously. Employing this methodology provides a unique avenue for acquiring insights into the mechanisms underlying *DCX* mutations, insights that are not attainable through overexpression or *DCX*-KO experiments.

Chapter 2: Materials and Methods

ES cell culture

ESCs were maintained on a monolayer of γ -irradiated mouse embryonic fibroblast feeder cells and passaged every 2–3 days. Cells were cultured at 37°C and 5% CO₂ in DMEM medium supplemented with 15% (v/v) fetal bovine serum, 20 mM HEPES (pH 7.4), 2 mM L-glutamine, 50 U/mL penicillin/streptomycin, 0.1 mM MEM non-essential amino acids, 50 μ M β -mercaptoethanol, and 500 U/mL recombinant mouse leukemia inhibitory factor.

Gene Editing

ESCs were plated in ESC medium (DMEM medium supplemented with 15% (v/v) fetal bovine serum, 20 mM HEPES (pH 7.4), 2 mM L-glutamine, 50 U/mL penicillin/streptomycin, 0.1 mM MEM non-essential amino acids, 50 μ M β -mercaptoethanol, 500 U/mL LIF) onto γ -IR inactivated mouse embryonic fibroblast (MEF) feeders. We generally started cells in one well of a 6-well plate in 4 mL of ESC medium. Cells were grown at 37 °C, 5% CO₂ in a standard tissue culture incubator. ESCs were passaged least once before nucleofection and fed 1-2 hours before. To prepare for nucleofection, mESCs were trypsonized and a single-cell suspension was generated. Cell suspension was added to a gelatinized 60-mm dish (pre-treated for at least 15 min with 0.2% (w/v) gelatin/DPBS) for at least 40 min (but not more than 1 h) to deplete the MEF feeder cells.

The targeting vector containing the Dcx-T203R mutation was linearized using the XhoI restriction enzyme. Alt-R CRISPR-Cas9 crRNA:tracrRNA was purchased from IDT

to target the *Dcx* locus with the guide RNA sequence being: CCAGTTCGTAAATGGGTCCT. Cas9/gRNA ribonucleoprotein complexes were assembled according to the IDT Alt-R protocol, then nucleofection was performed using the Amaxa 4D-nucleofector core unit with X unit and the P3 primary cell kit for ESC nucleofection, as described in (Dai et al. 2020). For each nucleofection, 2×10^6 ESCs were used.

Southern Blotting

Genomic DNA was prepared by lysing cells at 56°C overnight in lysis buffer (200 mM NaCl, 100 mM Tris-Cl pH 8.0, 5 mM EDTA, 0.2% SDS), supplemented with 0.2 – 0.4 mg/mL proteinase K, followed by precipitation and purification by phenol-chloroform-isoamyl alcohol extraction per standard protocols. DNA was digested with the indicated restriction enzymes, genomic fragments were separated by agarose gel electrophoresis, transferred to nylon membranes (Zeta-Probe GT, Bio-Rad), and hybridized overnight at 42°C with radiolabeled DNA probes per standard protocols. Membranes were washed the next day and then film was developed from probed membranes after 48 hours of exposure.

RNA isolation and cDNA transcript sequencing

RNA was extracted using an RNA extraction kit (Zymo Research). 500 ng of RNA was converted to cDNA using the High-Capacity cDNA Reverse Transcription Kit (Thermo Fisher) and the following settings: 25 °C for 10 min, 37 °C for 2 h, and 85 °C

for 5 min. One microgram of total RNA was used for cDNA synthesis using Superscript III Reverse Transcriptase and Oligo (dT) primers (Invitrogen, 18080093).

Neuronal Differentiation

To start the differentiations mESCs were transitioned from being grown on feeders to grown on gelatin-coated dishes (0.1% (w/v) gelatin). They were then maintained in ESC medium (500 mL knockout DMEM medium (Thermo Fisher Scientific, 10829018), supplemented with 10% fetal bovine serum (Sigma-Aldrich, F2442), 1x nonessential amino acids (Invitrogen, 11140050), 2 mM L-glutamine (Invitrogen, 25030081), 1x penicillin/streptomycin (Thermo Fisher Scientific, 15140122), 5×10^7 units LIF (Sigma-Aldrich, ESG1107). The cells were replated every other day. mESCs were differentiated to cortical neurons according to Gaspard et al., with modifications

Cells were switched to DDM (DMEM/F12, GlutaMAX (Thermo Fisher Scientific, 10565018) supplemented with 1x N2 supplement (Thermo Fisher Scientific, 17502048), 0.1 mM non-essential amino acids, 1 mM sodium pyruvate (Thermo Fisher Scientific, 11360070), 500 mg/ml BSA (Thermo Fisher Scientific, 15260037), (50 U/mL penicillin and streptomycin) on day 1 of differentiation. The medium was switched to N2/B27 medium (a mixture 1:1 of neurobasal/B27 medium (Neurobasal (Thermo Fisher Scientific, 21103049) supplemented with 1x B27 (Thermo Fisher Scientific, 12587010), 2 mM glutamine, 50 U/mL penicillin and streptomycin) and DDM) at day 10 and then left for the transition period until day 12. On differentiation day 12, 1.5×10^7 cells were replated on poly-L-lysine- and laminin-coated 100 mm dishes and maintained in N2/B27 medium. They were maintained until ready for further analysis (up to day 21).

maintained in N2/B27 medium. At this point, the cells were incubated with a readthrough drug (ataluren or G418), or with vehicle control (DMSO).

Statistics

To analyze data from imaging experiments, all statistics were carried out using Prism software.

Protein Extraction and Immunoblotting

Whole cell extracts were prepared from cells in ice-cold THB buffer (250 mM sucrose, 20 mM Tris pH 7.4, 1 mM EDTA, 1 mM EGTA), supplemented with protease inhibitors (cOmplete EDTA-free protease inhibitor cocktail, Roche) and 0.5 mM PMSF. Protein concentration was determined (Bio-Rad Protein DC assay), samples were briefly sonicated, 6x SDS sample buffer (0.5 M Tris-Cl pH 6.8, 30% (w/v) glycerol, 10% (w/v) SDS, 0.6 M dithiothreitol, 0.012% (w/v) bromophenol blue) was added to a final concentration of 1x, and samples were denatured by incubation at 95°C for three minutes. Equal amounts of protein were separated by SDS-PAGE, followed by immunoblotting with primary antibodies against Dcx (rabbit polyclonal, 1:10,000; ab18723, Abcam) and β III-tubulin (rabbit polyclonal, 1:20,000; ab18207, Abcam), Alpha tubulin antibody (rabbit polyclonal, 1: 5,000, Cell Signaling: 2144S), Spinophilin antibody (1: 5,000, rabbit polyclonal, Abclonal A6412).

Scratch Wound Assay

Differentiated neurons were seeded in 96-well Imagelock (for IncuCyte, Sartorius) at a density of 10,000 cells per well (100,000 cells/mL) and incubated overnight. An open wound area was created in the cell monolayer using the IncuCyte® Wound Maker tool. Cells were imaged after wounding every 2 h for a total duration of 50h using the IncuCyte live cell imaging system at 10X magnification. For each time point, relative wound closure was calculated using the Scratch Wound analysis pipeline of the Incucyte ZOOM™ software.

Tail Fibroblast Transfections

For assessment of DCX actions, SV40 Mouse Large T transformed tail fibroblasts were plated on 35mm glass bottom dishes that had previously been coated with 0.1% gelatin (P35G-1.5-14-C MatTek). They were plated sparsely at 50,000 cells per 35mm dish, to increase visual field while imaging. Transient transfections were performed overnight (12 hours) using TransIT-293 (Mirus, MIR 2700) according to the manufacturer's instructions with the corresponding plasmid. Medium was changed and live-imaging was carried out 72 hours after on an iSIM microscope.

Detergent Extraction

The detergent extraction assay was performed as described by Cohen et al (Cohen et al. 1997). Sub-confluent cultures of tail fibroblasts were grown on 10cm plates. They were washed once with PBS and then with MES buffer (50 mM MES pH 6.8, 2.5 mM EGTA, 2.5 mM MgCl₂). Cells were then extracted for 3 min with 0.5 ml of 0.5% Triton X-100 in MES buffer supplemented with protease inhibitors. The supernatant was collected and centrifuged for 2 min at 16 000 g at 4°C. The clear supernatant was then transferred to new tubes. Two volumes of cold ethanol were added to the tubes and incubated at -20°C overnight. The tubes were centrifuged for 10 min at 16,000 g at 4°C and resuspended in 200µl of 2× protein sample buffer without dye. The detergent-insoluble matrix (InSol) remaining on the plate was extracted in 200µl of 4× protein sample buffer (w/o Dye). It was then scraped from the plate with a rubber policeman and collected into tubes for further analysis.

Immunofluorescence

Transfected cells were plated on glass coverslips. After 48 h they were washed twice with phosphate-buffered saline (PBS), then fixed at room temperature and permeabilized simultaneously in 4% paraformaldehyde (PFA) for 15 min. After fixation the cells were incubated with blocking solution (PBS + 0.1 % triton-x + 5 % Donkey serum) then they were incubated in 30 µl of the first antibody for 60 min at room temperature, then washed three times with PBS and incubated for 30 min with 30 µl of fluorescent-conjugated secondary antibodies. The coverslips were washed three times

with PBS, drained and mounted. The immunostaining was visualized using the iSIM microscope (Objective and type of microscope).

Image Analysis

Image analysis was done using both Fiji and Image J depending on software version needed.

Chapter 3: Results

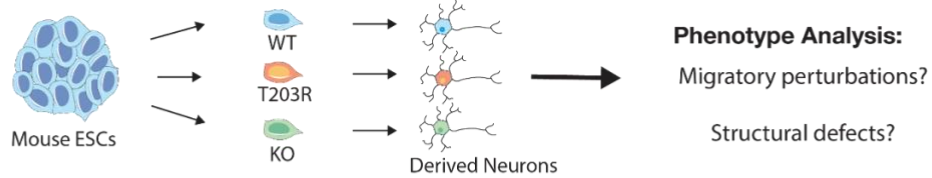
3.1 Dcx-T203R introduction via Gene Targeting

Until now studies of DCX function have focused on analyzing phenotypes associated with complete ablation of the DCX protein and have shown no cortical phenotypes in mouse models. However, the DCX sequence is 99.5% conserved between humans and mice making the examination of human disease-causing mutation possible in the mouse (Fig. 3.1B). Therefore, we planned to introduce a human disease-causing patient mutation in the *Dcx* endogenous locus of mouse embryonic stem cells (mESCs), followed by differentiation into neurons and analyzing phenotypes *in vitro* (Fig. 3.1A).

Alterations of the primary structure can affect protein stability. To address this, we first examined if the introduction of the disease-causing Dcx-T203R mutation impacts DCX protein expression levels. To do this, 293T cells were transfected with an overexpression plasmid containing either WT-Dcx or T203R-Dcx and western blot analysis was performed 48 hours after the transfection to determine the Dcx protein expression for both conditions. We found that mutant Dcx-T203R protein is expressed at a similar, albeit slightly lower, level than WT-Dcx (Fig. 3.2).

To rigorously test the implications of the human mutation on protein function, we used a gene editing approach that combined homologous recombination and *Clustered Regularly Interspaced Short Palindromic Repeats* (CRISPR)/Cas9 to introduce the T203R mutation at the endogenous *Dcx* locus (Dai et al. 2020). By introducing a mutation identified in humans (DCX-T203R) at a site in the endogenous mouse *Dcx* locus that is fully conserved in mouse, I can analyze the phenotypes seen in human cortical development and thus begin to elucidate how *Dcx* mutations alter its function in migrating neurons.

A



B

<i>M. musculus</i>	1	MELDFGHFDERDKA	SRNMRGSRMNGLPSPTHSAHCSFYRT	40
<i>H. sapiens</i>	1	MELDFGHFDERDKT	SRNMRGSRMNGLPSPTHSAHCSFYRT	40
<i>M. musculus</i>	41	RTLQALSNEKKAKKVRFYRNGDRYFKGIVYAVSSDRFRSF	80	
<i>H. sapiens</i>	41	RTLQALSNEKKAKKVRFYRNGDRYFKGIVYAVSSDRFRSF	80	
<i>M. musculus</i>	81	DALLADLTRSLSDNINLPQGVRYIYTDGSRKIGSMDELE	120	
<i>H. sapiens</i>	81	DALLADLTRSLSDNINLPQGVRYIYTDGSRKIGSMDELE	120	
<i>M. musculus</i>	121	EGESYVCSSDNFFKKVEYTKNVNPNWSVNVKTSANMKAPQ	160	
<i>H. sapiens</i>	121	EGESYVCSSDNFFKKVEYTKNVNPNWSVNVKTSANMKAPQ	160	
<i>M. musculus</i>	161	SLASSNSAQARENKDFVRPKLVTIRSGVKPRKAVRVLN	200	
<i>H. sapiens</i>	161	SLASSNSAQARENKDFVRPKLVTIRSGVKPRKAVRVLN	200	
<i>M. musculus</i>	201	KK [*] AHSFEQVLTDITEAIKLETGVVKKLYTLDGKQVTCLH	240	
<i>H. sapiens</i>	201	KK [*] AHSFEQVLTDITEAIKLETGVVKKLYTLDGKQVTCLH	240	
<i>M. musculus</i>	241	DDFGDDVFIACGPEKFRYAQDDFSLDENECRVMKGNPSA	280	
<i>H. sapiens</i>	241	DDFGDDVFIACGPEKFRYAQDDFSLDENECRVMKGNPSA	280	
<i>M. musculus</i>	281	AGPKASPTPQKTSAKSPGPMRRSKSPADSGNDQDANGTS	320	
<i>H. sapiens</i>	281	AGPKASPTPQKTSAKSPGPMRRSKSPADSGNDQDANGTS	320	
<i>M. musculus</i>	321	SSQLSTPKSKQSPISTPTSPGSLRKHKVDLYLPLSLDDSD	360	
<i>H. sapiens</i>	321	SSQLSTPKSKQSPISTPTSPGSLRKHKVDLYLPLSLDDSD	360	
<i>M. musculus</i>	361	SLGDSM	366	
<i>H. sapiens</i>	361	SLGDSM	366	

Figure 3.1: Experimental Overview

(A) Schematic of workflow for the introduction of *Dcx*-T203R into the mouse endogenous *Dcx* locus, generating either WT, DCX KO, or T203R mutant mESCs. Mouse ESCs were then used to derive neurons and further phenotypic analysis was conducted. **(B)** Protein alignment of human and mouse doublecortin showing 99.5% conservation, allowing for the disease-causing mutation T203R (highlighted in red) to be recreated in the mouse genetic background.

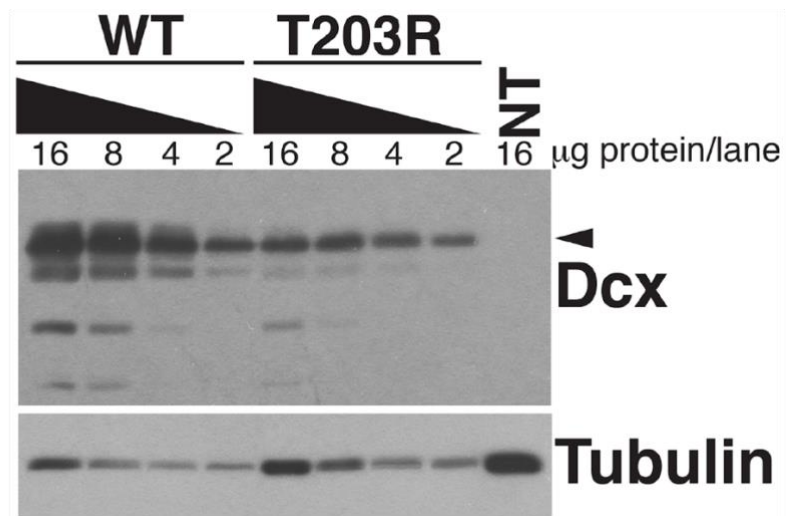


Figure 3.2: DCX T203R Expression Upon Transient Transfection

293T cells were transiently transfected with expression vectors encoding either wildtype (WT) Dcx or Dcx T203R. The indicated amounts of total protein from whole cell extracts were analyzed by immunoblotting with antibodies to DCX or alpha-tubulin as a loading control. The arrowhead points to the band corresponding to full-length Dcx. NT, not transfected.

Introduction and validation of *Dcx*-T203R mutation into mouse endogenous locus

To mechanistically investigate the phenotypes seen in patients with mutant *DCX*, I needed to generate a mouse embryonic stem cell (mESC) line that contained a mutation at the mouse endogenous locus. First, the targeting vector was generated containing the *Dcx*-T203R mutation as well as a neomycin selection cassette and BamHI restriction site, flanked by two homology arms (Fig. 3.3). The BamHI restriction site was added to the targeting vector in order to make screening *via* restriction digest a way to distinguish targeted and WT alleles in an effective way. Initial targeting was done by “classical” methods involving the electroporation of the linearized targeting vector into mESCs, which would allow for homologous recombination to occur and introduce the mutation into the *Dcx* locus. After nucleofection, the mESCs were plated sparsely and treated with G418 to undergo selection for clones with the insertion of the targeting vector. We screened genomic DNA that was extracted from 384 stem cell clones that were picked after selection via long-range polymerase chain reaction (LR-PCR) across both the 3’ and 5’ homology arms and into the endogenous locus. However, we did not detect knock-in events by long-range PCR and decided to attempt a different targeting approach.

In order to enhance gene targeting efficiency, we decided to utilize CRISPR/Cas9 technology in combination with the targeting vector nucleofection and homologous recombination. Specifically, we utilized CRISPR ribonucleoproteins (RNPs), which provide transient DNA cutting, to introduce a DNA double-strand break (DSB) at the *Dcx* endogenous locus. This would enhance homologous recombination

with the linearized targeting vector and improve gene targeting outcomes at the *Dcx* locus. In order to carry this out, we first designed a guide Ribonucleic acid (gRNA) that would cut at the endogenous *Dcx* locus but did not also cause CRISPR/Cas9-induced DSBs within the targeting vector.

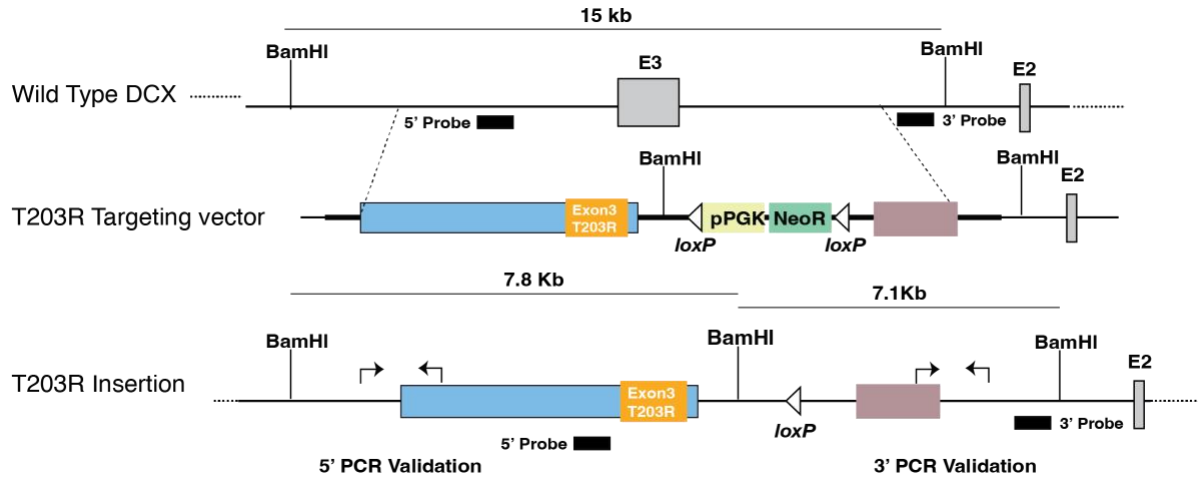


Figure 3.3: Introduction of Dcx-T203R Mutation at Endogenous Locus

Schematic of gene targeting of *Dcx* in the mouse endogenous locus, using a targeting vector containing *Dcx*-T203R mutation in exon 3 along with a *Bam*HI restriction enzyme cut site and a neomycin selection cassette.

The ribonucleoprotein (RNP) complexes were formed, which contain the Cas9 protein as well as the gRNA which was designed to target the Dcx locus at exon 3. This location was chosen based on the proximity to where insertion of the targeting vector should take place. Per nucleofection 2×10^6 cells were nucleofected with the RNPs and then resuspended in 10mls of medium. After nucleofection, 9mls of the mESCs from the resuspension were plated onto a 10cm² dish. The sparsely plated cells then underwent selection via G418 introduction into the medium to prepare for picking and isolating targeted clones. There were 1,024 mESC clones picked and validated for correct integration of the targeting vector.

The first set of validation experiments were conducted using 5'- and 3' LR-PCR (Fig. 3.4A). All clones were analyzed and only those with both 3' and 5' LR-PCR accurate band sizes moved forward to be validated via Southern blot analysis (Fig. 3.4B). The Southern blot validation consisted of probing with the 3' Southern probe and 5' Southern probe in sequential order. Two targeted clones were positively validated by PCR and Southern blot (Fig. 3.4C). Then the floxed selection cassette was deleted via transient, adenoviral expression of Cre recombinase. The two clones were then validated for proper selection cassette deletion by PCR analysis as well as another Southern blot. To finalize the validation of the complete deletion of the selection cassette, a Southern blot was carried out and the Neo probe was used to determine the absence of the selection cassette.

The validated clones were then differentiated into neurons using the protocol discussed in the following section. RNA was extracted from WT and T203R-5F and T203R-7C neurons, then complementary DNA (cDNA) for the Dcx transcript was amplified and sent out for sequencing. Sequencing showed the insertion of only a single mutation at Dcx-T203R in neurons derived from targeted mESCs (Fig. 3.5).

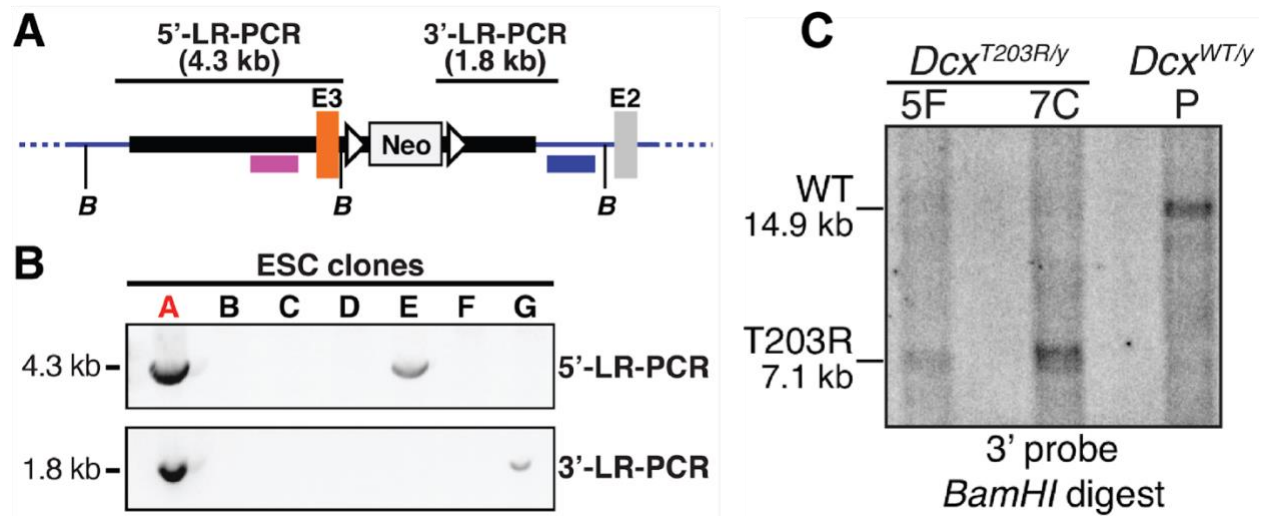


Figure 3.4: Validation of T203R Knock-in mouse ESCs

(A) Schematic of the endogenous *Dcx-T203R* knock-in locus. Long-range PCR (LR-PCR) strategies to detect correct targeting are shown. Location of 5'- and 3'-probes for validation by Southern blotting are shown (pink and blue boxes). B, *Bam*HI restriction sites. **(B)** Example of a correctly targeted embryonic stem cells (ESC) clone (A). Non-targeted clones (B-D, F) and clones only targeted on one end (E, G) are shown for comparison. Clones were analyzed with the LR-PCR strategies shown in (A). **(C)** Southern blot of targeted clones 5F and 7C that were previously validated by LR-PCR. Properly targeted clones show a single band at 7.1 kb vs. WT band at 14.9 kb.

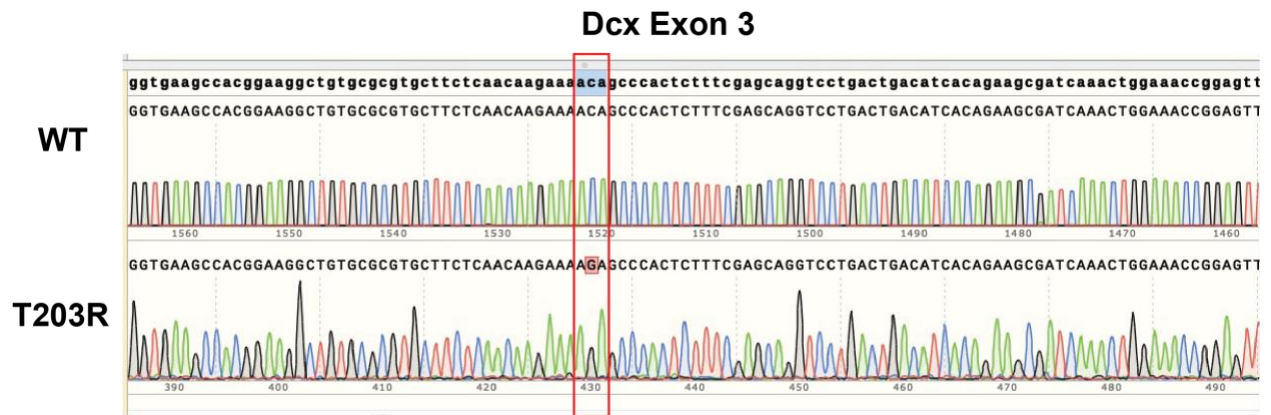


Figure 3.5 Sequencing of Dcx cDNA Transcript

Sanger sequencing of Dcx cDNA transcript at exon 3 from Dcx-WT and Dcx-T203R 5F clone derived neurons. Top shows WT sequence (ACA) and bottom shows insertion of Dcx-T203R mutation (sequenced changed to (AGA) 5F clone neurons.

3.2 Targeted mESC Neuronal Differentiation

Optimization of neuronal differentiation of targeted mESCs

To examine the cell-intrinsic impact of *Dcx* mutation or complete ablation on cell migration, dynamic localization of *Dcx* and morphological differences that arise in mutant neurons. Through several in-vitro assays, a neuronal differentiation protocol had to be optimized for use with the gene targeted mESCs. Both validated *Dcx-T203R/Y* clones (*Dcx* 5F and *Dcx* 7C), as well as *Dcx*^{-/Y} and *Dcx*^{+/Y} (*Dcx*-WT) were included in the differentiations.

First, neuronal induction was attempted by ectopic overexpression of a Neurogenin 2 (NGN2)-containing plasmid in the targeted mESCs. NGN2 is a neuronal basic helix-loop-helix transcription factor whose ectopic expression has been shown to induce neuronal differentiation of mESCs (Lin et al. 2021; Thoma et al. 2012). However, in our hands, neurons failed to be produced reliably and efficiently from overexpression of NGN2 [data not shown], so we moved to a directed differentiation approach, as described below.

Directed differentiation approaches guide neural induction and maintenance of mESC cultures through culture conditions involving specific factors and substrates (Mao and Zhao 2020; Vanderhaeghen 2012). We chose an approach utilizing a dual SMAD signaling inhibition strategy that channels differentiation toward the dorsal lineage (Gaspard et al. 2009). However, during the course of the experiments it became obvious that several key aspects needed to be adjusted and optimized to robustly and

reliably derive forebrain neurons. First, mESCs were grown up in serum-free medium, then plated sparsely and transitioned into a defined default medium (DDM), (“Early Differentiation”, Fig. 3.6). The original protocol involved the use of cyclopamine, but we observed a decrease in neural progenitor quality with its addition. As a result, we removed cyclopamine from the protocol. In our modified protocol, cells were maintained in DDM for ten days, at which time the culture was mainly composed of neural progenitor cells. On day 10 the cells were changed into N2/B27 medium which contains B27 without vitamin A, which has the capacity to be turned into retinoic acid (RA) and decrease rostral forebrain identities. Cells were maintained like this until day 12 (“Transition”, Gaspard et al. 2009, Fig. 3.6). The additional transition time in N2/B27 before replating the cells greatly improved the neuron’s survivability in culture and resulted in higher neuron yield by the end of the protocol. At day 13, the cells were then sparsely replated, 80k cells total per coverslip, on poly-D-lysine/laminin-coated coverslips, and maintained until day 21 in N2/B27 medium, (“Late Differentiation”, Fig. 3.6). By the end of the differentiation protocol at day 21, we consistently observed that upwards of 80% of cells in culture are excitatory neurons.

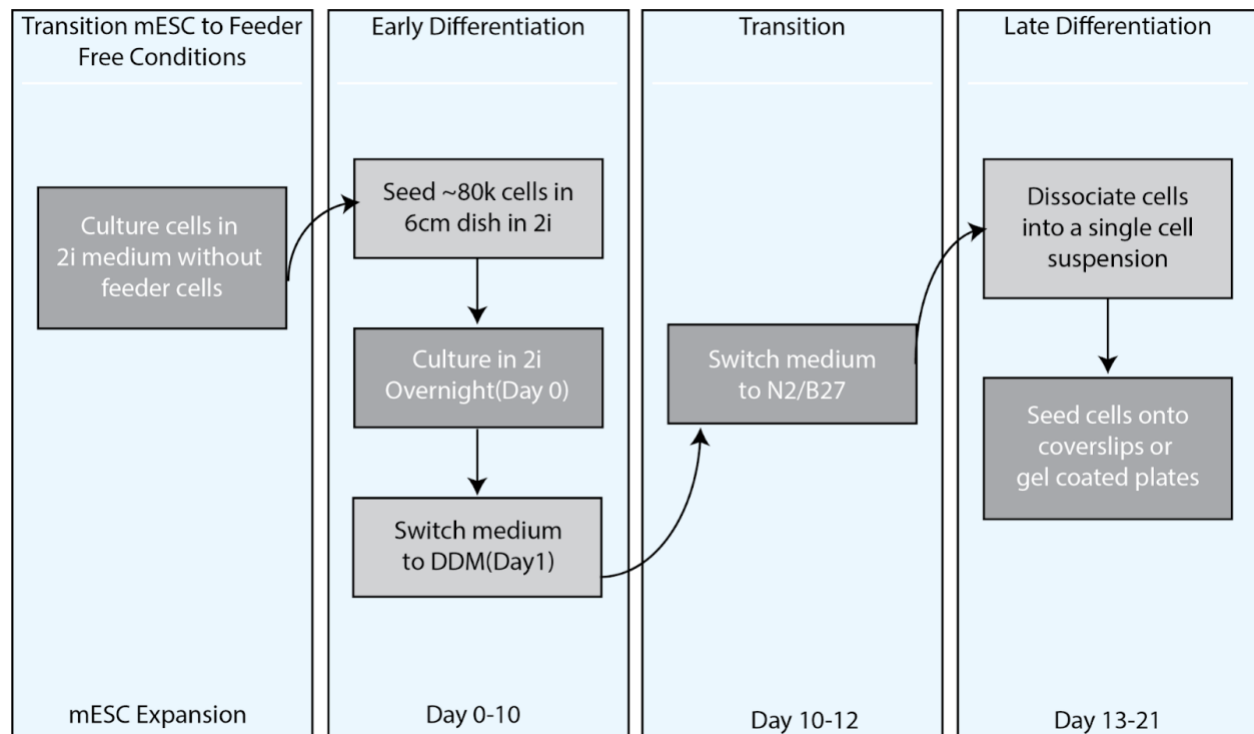


Figure 3.6: Neuronal Differentiation Protocol Schematic

Overview of the periods of neuronal induction broken down into early and late differentiation stages. mESCs begin in 2i medium without feeder cells and then are changed to DDM. Cyclopamine had normally been used in differentiation protocols, but was removed from DDM medium here to increase derivation of dorsal telencephalic excitatory neurons. This marks early differentiation and neural induction. Neurogenesis starts at approximately day 6 and continues until the end of the protocol at day 21. Cells left in culture for longer than day 21 will go through a wave of gliogenesis. At around differentiation day 10-12 the cell culture contains a majority of progenitors and neurons which then need to be transitioned into N2/B27 medium for late differentiation. This transition period was introduced to the workflow and resulted in higher viability of neurons and a more reproducible protocol overall. The cells are then seeded onto poly-D-lysine/laminin-coated coverslips in N2/B27 media at day 13 and maintained until day 21. (Modified from Gaspard et. al. 2009)

Composition and Maturation of Derived Neurons

To comprehensively evaluate the composition of cell types within our cultured samples upon completion of the differentiation protocol, we employed immunofluorescence (IF) microscopy. This approach utilized a careful selection of specific markers to distinguish and identify distinct cell types. Specifically, for the differentiation of neurons, astrocytes, and oligodendrocytes, we strategically chose antibodies against known marker proteins. Specifically, the antibody targeting Dcx was utilized to detect immature neurons, while Glial fibrillary acidic protein (Gfap) antibodies as well as overall cell morphology were employed to identify astrocytes. Furthermore, we utilized Oligodendrocyte transcription factor 2 (Olig2) antibodies to assess the presence of oligodendrocytes. This not only allowed us to discern the presence of these different cell types but also provided valuable insights into the overall composition of our cultured cells, facilitating a comprehensive analysis of the outcomes of the differentiation experiments.

Cells were counted based on marker expression and morphology, and the percentages of cells expressing either Dcx, GFAP or Olig2 were quantified for three separate differentiations derived from Dcx wildtype (WT), T203R mutant (Clones 5F and 7C), and Knockout (KO) mESCs (Fig. 3.7D). After quantifying the proportion of Olig2 positive cells in culture, we observed that the distinctions among the different Dcx genotypes were minimal and lacked statistical significance as each fell within the range of 3-5% of cultured cells across all samples (Fig, 3.7A). The expression of GFAP in cultured cells demonstrated a slight increase when comparing the WT and the two

mutant clones; however, this increase did not reach statistical significance. In contrast, a notable and statistically significant alteration in GFAP expression was observed when comparing WT to the KO cell line, with WT cultures having roughly 10% GFAP expressing cells in culture while the KO cell cultures displayed nearly 30% of cells expressing this marker (Fig. 3.7B). There was no significant variation in the proportion of cells expressing the neuronal marker Dcx when comparing the WT cells to the two Dcx-T203R mutant clones (Fig. 3.7C). Overall, these results show that the neuronal differentiation culture composition was not significantly different between each of the samples.

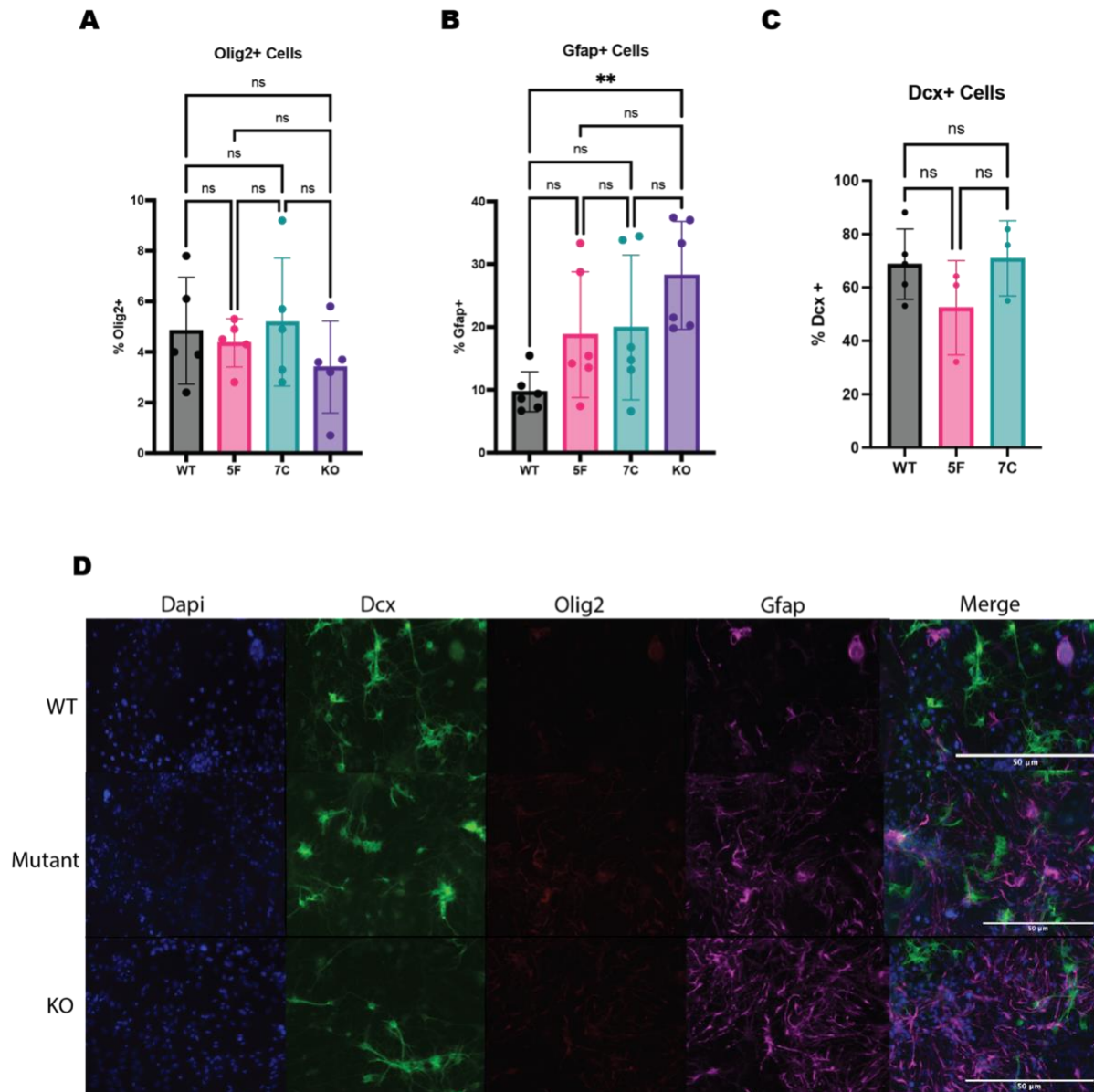


Figure 3.7: Cell Type Composition of Differentiation Culture

(A) The percentage of cells in the neuronal differentiation culture at day 21 that express Olig2 quantified using a one-way ANOVA. The expression of Olig2, which is an Oligodendrocyte marker, does not show any significant variation between cells derived from Dcx WT-, T203R-, or KO mESC cells (B) The percentage of cells in the neuronal differentiation culture at day 21 that express Gfap. There were some slight changes in expression of Gfap, with WT cells having the lowest proportion of cells expressing the marker, and slightly higher expression for mutant cells. However, there was a significant increase in expression of Gfap in KO cells when compared to WT using a one-way ANOVA analysis and Tukey test, $P = 0.0161$. (C) The percentage of cells in the neuronal differentiation culture at day 21 that express Dcx. There were no significant changes in expression of Dcx between WT, mutant or KO neurons, as shown using a one-way ANOVA analysis.

Next, IF microscopy was used to investigate the regional identity of cells in culture at two different time points within the neuronal differentiation to assess any differences in timing that would need to be taken into account when comparing the neurons. The early differentiation timepoint (Day 16) and late differentiation timepoint (Day 21) were chosen based on the previous study that the protocol was adapted from (Gaspard et al. 2009). Pax6 is a transcription factor that is important during the development of the central nervous system, and is expressed by neural progenitor cells during cortical development (Zhang et al. 2010; Sansom et al. 2009). Therefore, we expected the expression of Pax6 to decrease as differentiation advanced and the late time point to have few Pax6-positive cells. There were no significant differences in Pax6 expression between WT, both T203R mutant clones, and KO cells at the early time point, with all samples having 30-40% Pax6 expression (data not shown). The late time point saw some variation in Pax6 expression between genotypes. These variations were not statistically significant, except when comparing the late time point of mutant clone 5F and KO cells (data not shown). However, overall, among the neuronal differentiations, there weren't drastic differences of Pax6 expression at either time point which was expected.

Another marker that was analyzed was Forkhead Box G1 (Foxg1), which is a transcription factor that is specific to the telencephalon (Liu et al. 2022; Hou et al. 2020). Foxg1 expression was not expected to be changed due to Dcx mutation or Dcx KO, and after analysis of the neuronal differentiation cultures, this was confirmed (Fig. 3.8A). At the early differentiation time point all cultures expressed higher levels of Foxg1 expression, ~50%, than at the late timepoints where expression fell below 30% (Fig. 3.8B). This data shows that Dcx absence or mutation does not alter the proportion of cells that are Foxg1 positive during the length of the neuronal differentiation and the expression levels are similar among cells derived from mESCs of the indicated genotypes.

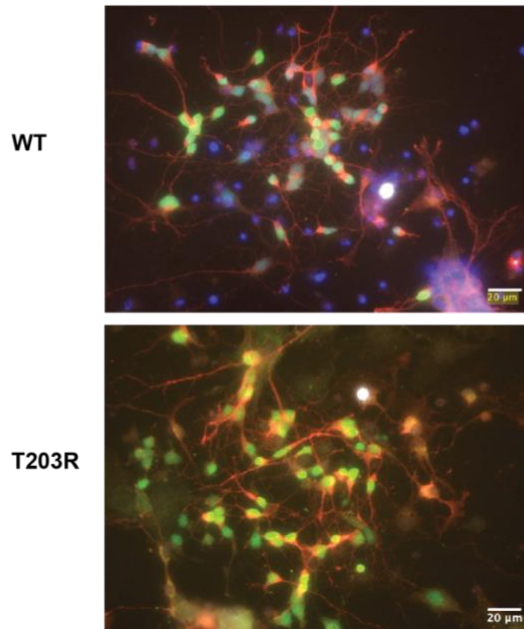
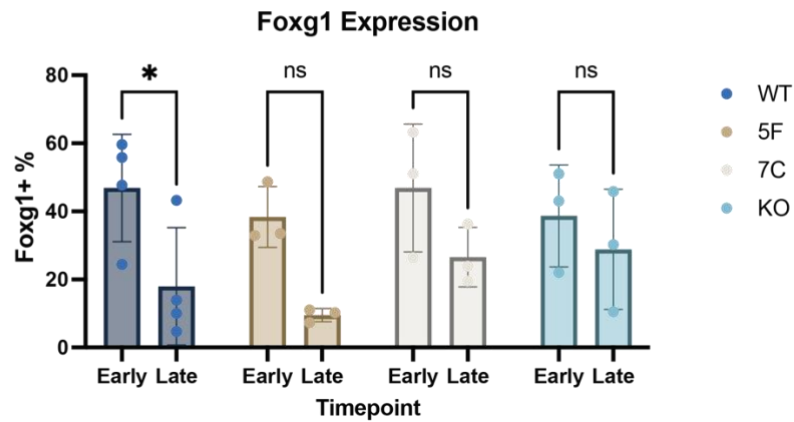
A**B**

Figure 3.8: Neuronal Differentiation Quantification of Regional Marker Foxg1

Two time-points were taken into account: the **Early** time-point at Day 16 in the early differentiation stage and the **Late** time-point at differentiation day 21, which is at the end of the late differentiation stage. Four cell culture conditions were analyzed: WT, two Dcx-T203R mutant subclones (5F and 7C), and the Dcx-KO cell lines. **(A)** Immunofluorescence images of differentiated neurons at final day(d21) of differentiation, showing expression of markers: Dcx- Red, Foxg1- Green, and Dapi (nuclear stain)- Blue. **(B)** The percentage of cells which express Foxg1 at neuronal differentiation culture day 21 was analyzed using a two-way ANOVA and Tukey test for multiple comparisons and no significant difference was noted among conditions at both time-points. Each dot represents the mean from one differentiation experiment. ns, not significant.

Aggregate formation

During the IF microscopy analysis of the derived neurons, notable Dcx-positive aggregates were identified in the soma and dendrites of Dcx-T203R mutant neurons. To investigate these aggregates further, neurons were also stained with Spinophilin (Spn) as previous findings indicate that Dcx mutant neurons form aggregates containing Spn (Bielas et al. 2007; Yap et al. 2016). T-brain-1 (Tbr1)-positive neurons were selected for analysis of either Spn or Dcx positive aggregates because Tbr1 is a marker of excitatory projection neurons (Bedogni et al. 2010; Fazel Darbandi et al. 2018). Notably, most aggregates were co-labeled with both Spn and Dcx in T203R mutant neurons (Fig. 3.9). Although it at much lower frequency, Dcx-KO neurons were also seen to contain Spn-positive aggregates (Fig. 3.9). Quantitative analysis of multiple differentiations showed that there was a significant increase in aggregate formation in T203R mutant neurons. Specifically, about 40% of the T203R mutant Tbr1+ neurons contained aggregates, whereas WT Tbr1+ neurons contained no aggregates (Fig. 3.10A).

However, the differences in the fraction of aggregate-containing Tbr1+ neurons between Dcx-WT and Dcx-KO neurons were not significant. There were also notable differences in neuronal morphology and size between WT and mutant neurons that may have been the result of the mutation. This observation should be further investigated. It also needs to be noted that in mutant neurons with aggregates, there was an average of roughly 4 large aggregates within each soma (3.10B). A closer look at the Spn+, Dcx+ aggregates can be seen in the soma of the two mutant clones, 5F and 7C (Fig. 3.10C).

These aggregates may be localizing to the nucleus for degradation or it may be due to another mechanism that should be further investigated.

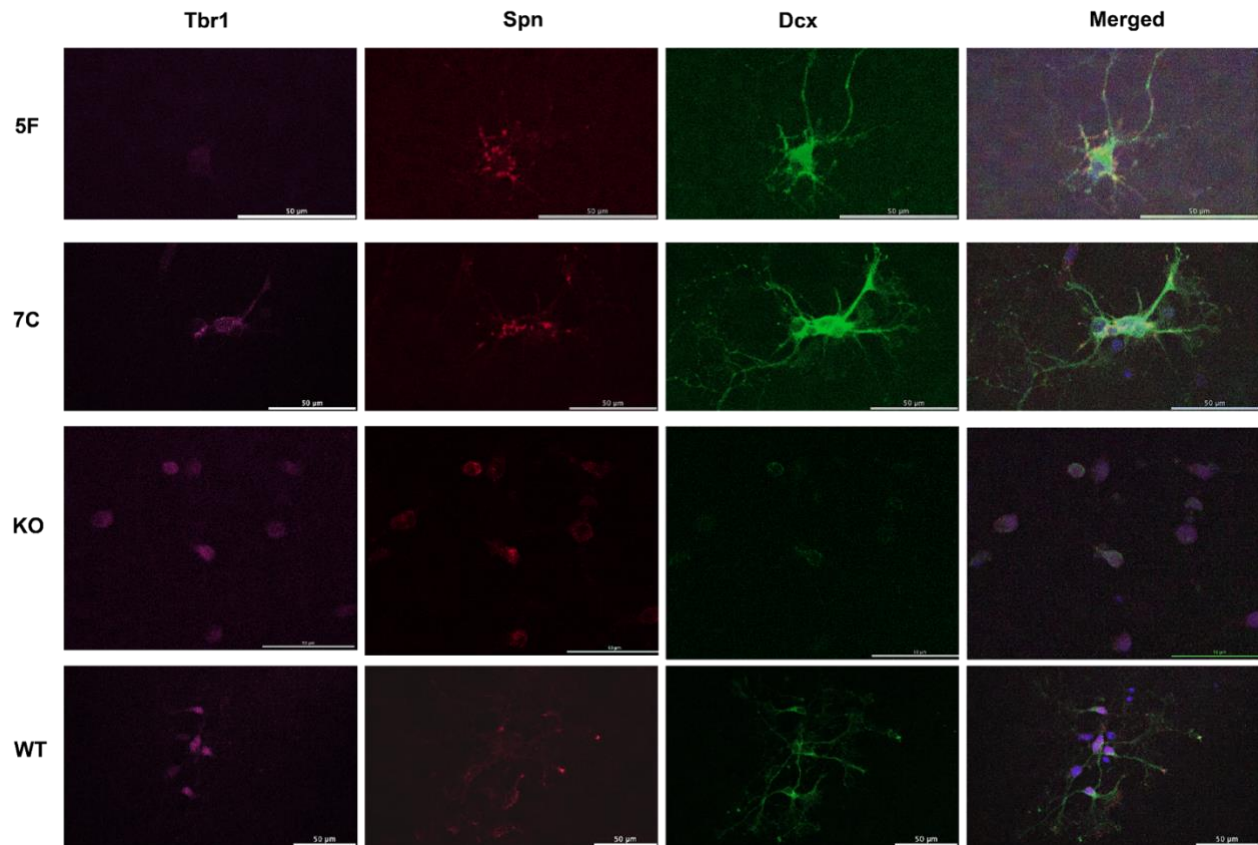


Figure 3.9: Derived Neurons Immunofluorescence

Neuronal differentiation cultures were plated on coverslips at Day 21. Neurons were identified through expression of Tbr1 and then analyzed for Dcx and Spn expression. A substantial amount of Tbr1+ Dcx-T203R (both mutant sub-clones: 5F and 7C) neurons had Spn aggregates in the soma that colocalized with Dcx. The Spn+ Dcx+ aggregates that were seen in the nucleus of mutant cells, were completely absent in WT neurons.

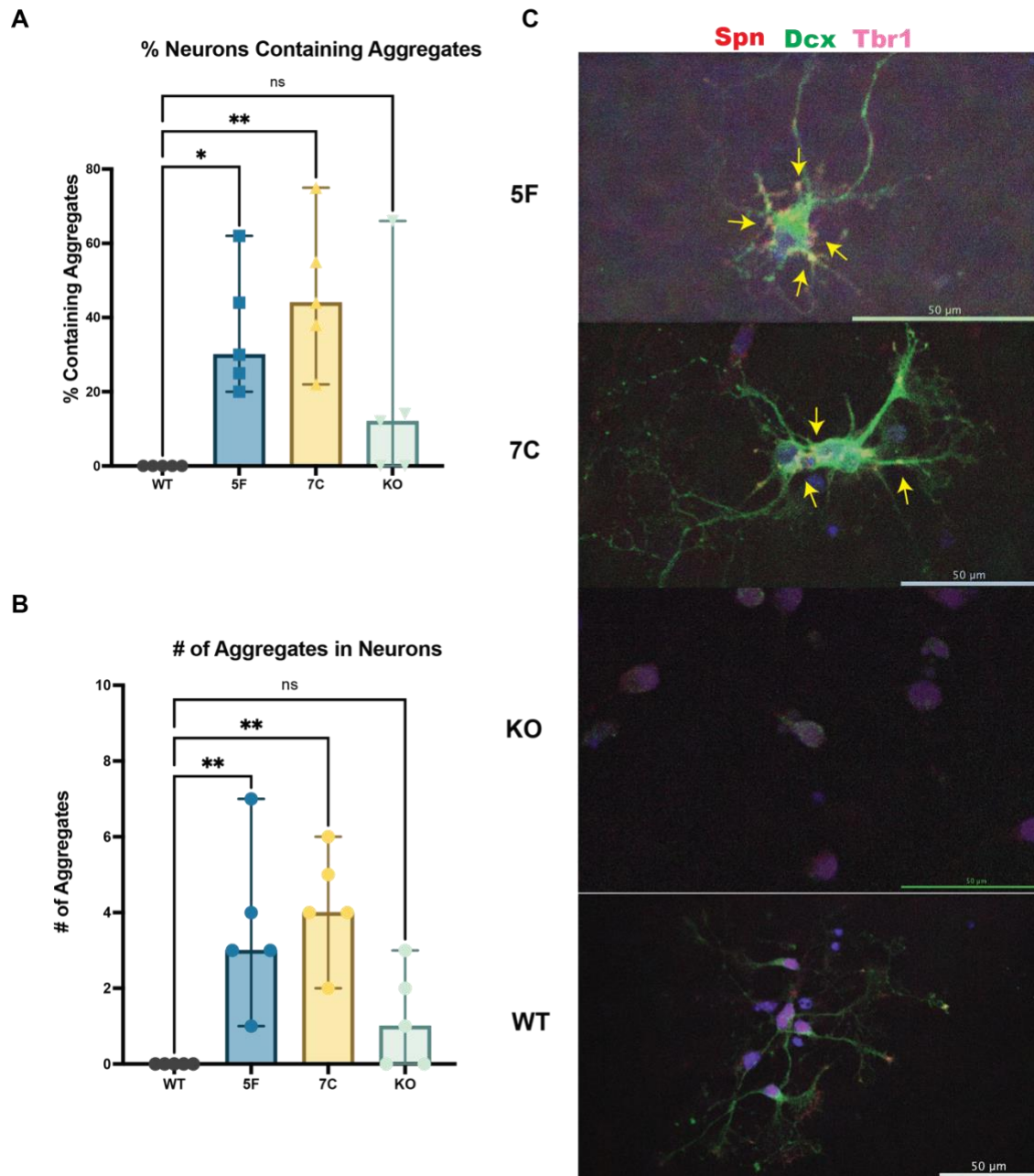


Figure 3.10: Spn and Dcx Aggregates in Derived Neurons

(A) Tbr1+ neurons that contained Spn+ aggregates were counted across all differentiations and the proportion of neurons containing aggregates in culture was quantified by one-way ANOVA comparing to WT cultures. Each dot on the graph represents the mean neurons containing aggregates per differentiation carried out **(B)** Of the neurons that did have aggregates, the number of aggregates found in their soma was counted and quantified by one-way ANOVA comparing to WT cultures. Each dot on the graph represents mean number of aggregates in neurons of distinct differentiations. **(C)** Immunofluorescence of derived neurons showing the aggregates found in mutant clones 5F and 7C are highlighted with yellow arrows which are absent in WT neurons.

Impact of Dcx mutations on neuronal migration

To investigate the impact of the Dcx-T203R knock in mutation on neuronal migration, a scratch-wound assay was conducted. mESC-derived neurons were plated in a 96-well plate, and a scratch was created at the bottom of each well. Subsequently, images were captured every two hours for a duration of 48 hours to monitor the migration of neurons into and within the scratch. Comparing the derived neuronal cultures of Dcx-WT to those of Dcx-T203R cells revealed notable differences in migration dynamics. Initially, upon the initiation of the experiment, it became evident that WT cells exhibited a significantly faster rate of migration into the scratch area. Remarkably, at the end of the 48-hour observation period, the WT cells had achieved four times the confluence within the scratch area compared to the T203R mutant cells. This observation underscores the complexities associated with migration for the mutant cells (Fig. 3.10A).

Furthermore, we extended the scope of the migration assay to compare not only WT and mutant cells but also to analyze the migration of Dcx-KO cells. The neuronal cultures of Dcx-KO mESCs were derived using the same protocol as WT and T203R mutant cells, and the migration assay was again conducted over a 48-hour timeframe. Once more, it became evident that WT cells exhibited a higher rate of migration into the scratch area when compared to both mutant and KO cells (Fig. 3.10B). Mutant T203R cells displayed the lowest scratch confluence at the conclusion of the experiment, while KO cells exhibited approximately 10% higher confluence at the 48-hour mark compared to mutant cells (Fig. 3.10B). However, it is noteworthy that even the KO cells only

achieved 30% scratch confluence in contrast to the approximately 70% confluence observed with WT cells (Fig. 3.10B). Therefore, although Dcx-KO cells exhibited better migration capabilities than Dcx-T203R cells, mutant cells demonstrated significantly reduced migration levels when compared to Dcx-WT cells. We note that these experiments were only done with one (clone 5F) Dcx-T203R mutant and further studies are required to repeat these studies with cells derived from the other Dcx-T203R mutant. However, the observed reductions in migration may have direct implications for the migration defects observed *in vivo*, underscoring the importance of understanding the impact of the Dcx mutation on neuronal migration at the endogenous level.

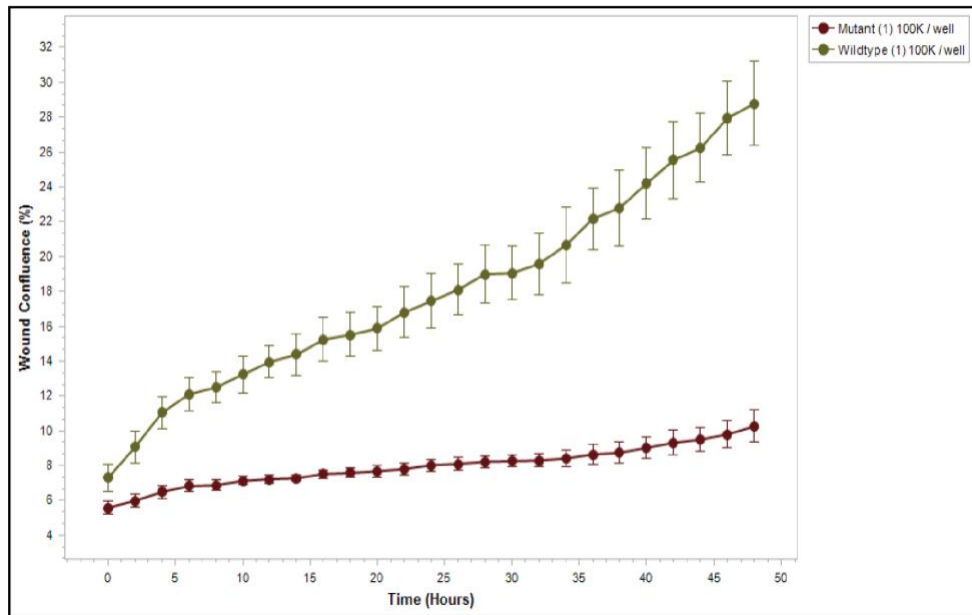
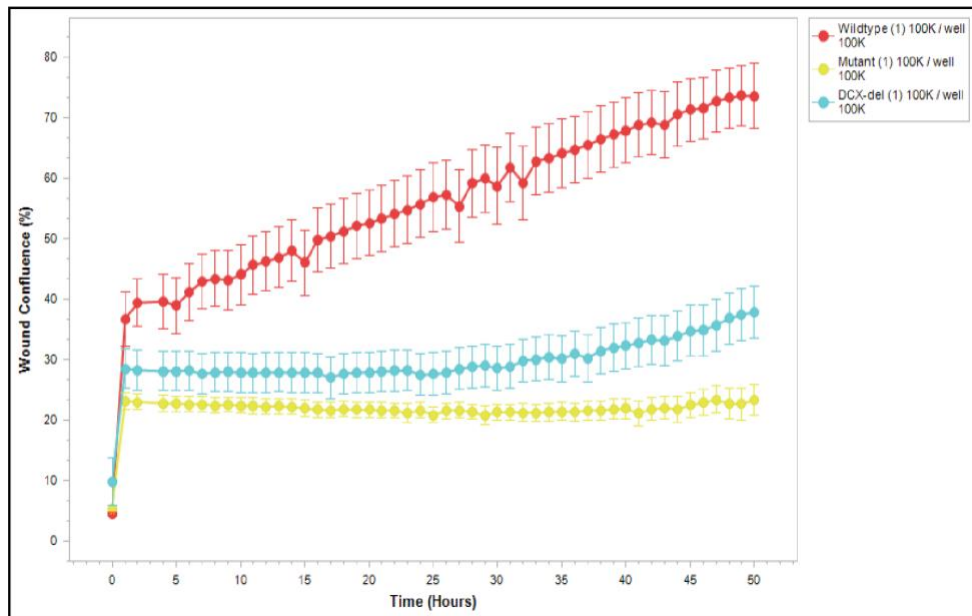
A**B**

Figure 3.11: Neuronal Migration Assay

(A) Initial migration assay was set up to evaluate the migration into the scratch wound between only Dcx-WT cells and Dcx-T203R Mutant cells from clone 5F. The Sartorius Incucyte® Scratch Wound Assay was used and analysis was done using Incucyte® Scratch Wound Analysis Software Module. (B) The samples used for the migration assay were expanded to include; Dcx-WT, Dcx-T203R and Dcx-KO derived neuronal cultures. Each dot represents the mean wound confluence of 48 wells for any given timepoint.

3.3 Dcx T203R MT binding dynamics

Dcx binding and aggregate formation

Dcx binding along MTs and its function on cytoskeletal structuring is an important component of the mechanics behind neuronal migration (Bechstedt and Brouhard 2012; Gleeson et al. 1999; Moores et al. 2004; Ettinger et al. 2016; Tanaka, Serneo, Higgins, et al. 2004; Tanaka, Serneo, Tseng, et al. 2004). Therefore, the introduction of the T203R mutation into the Dcx could potentially disrupt and alter normal Dcx binding along MTs. Dcx has also been shown to inhabit a particular zone along MTs which excludes the growing + ends, which are bound by end-binding protein 1 (EB1) (Ettinger et al. 2016). In order to examine Dcx-T203R vs. Dcx WT binding along MTs, mouse tail fibroblasts—which do not endogenously express Dcx—were transfected with either a Dcx-WT- or Dcx-T203R-expressing plasmid (pLenti6-DCX-EGFP), which had been used in a previous study (Ettinger et al. 2016). Originally, these plasmids contained the open-reading frame of human DCX, which was replaced with either mouse Dcx-WT-EGFP or mouse Dcx-T203R-EGFP for these experiments.

Immediately, noticeable disparities emerged in Dcx binding levels along MTs when comparing the T203R mutant and WT conditions. Specifically, fibroblasts transfected with Dcx-WT-EGFP exhibited considerably higher levels of EGFP fluorescence along MTs in contrast to those transfected with Dcx-T203R-EGFP (Fig. 3.11A). A comprehensive analysis across multiple independent transfections revealed that Dcx-WT-EGFP displayed an approximate 30% increase in mean fluorescence intensity along MTs compared to Dcx-T203R-EGFP (Fig. 3.11B). Furthermore, beyond

the intensity of binding, distinct Dcx-positive aggregates were exclusively observed in cells transfected with Dcx-T203R-EGFP (Fig. 3.11C). Notably, these mutant Dcx aggregates bore a striking resemblance to the aggregates previously observed in neurons derived from the mutant mESCs (Fig. 3.9).

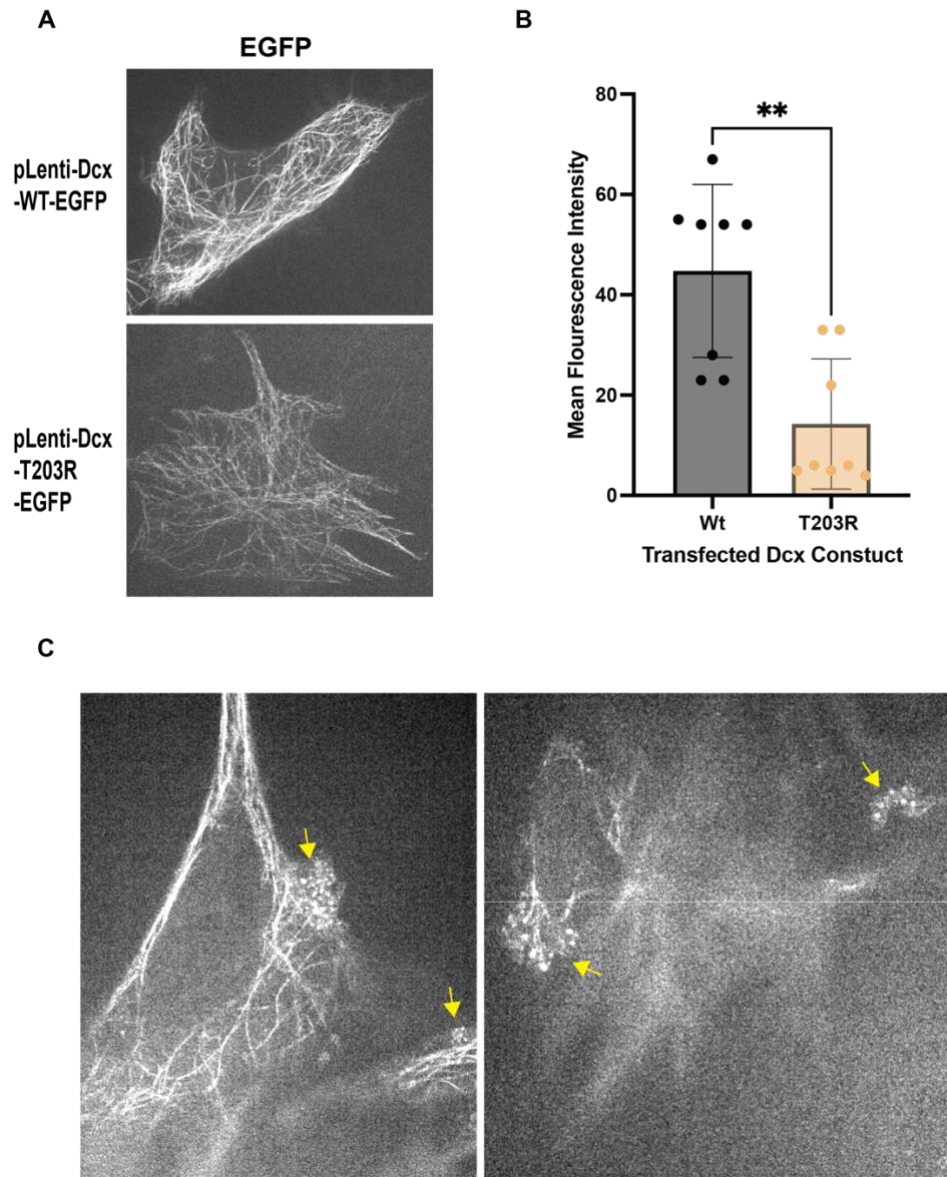


Figure 3.12: Dcx binding Intensity in Transfected Fibroblasts

(A) Live imaging of mouse tail fibroblasts transfected with either Dcx-WT-EGFP or Dcx-T203R-EGFP showing differences in binding intensity along MTs. **(B)** Quantification of the mean fluorescence intensity of Dcx-EGFP along MTs was carried out using an unpaired, two-tailed t-test, $P = 0.0013$ (**). Each dot represents the mean of independent separate experiments. **(C)** Dcx-EGFP-positive aggregates were seen in the cells transfected with the Dcx-T203R-EGFP mutant construct and are highlighted with yellow arrows.

Dcx and Eb1 binding zones

Next, we sought to investigate if the introduction of Dcx-T203R disrupted the mutually exclusive zones along MTs that Dcx and Eb1 inhabit, as described in a previous study (Ettinger et al. 2016). The original EB1 Δ C-mCherry plasmid was co-transfected with either pLenti6-Dcx-WT-EGFP or pLenti6-Dcx-T203R-EGFP. Live imaging of the cells showed the mutually exclusive zones of binding along the MTs are conserved in the cells transfected with mutant Dcx (Fig. 3.13). At this level of analysis there was no noticeable change in MT dynamic restructuring within mutant cells when compared to WT cells. Although more detailed studies are needed to further quantify the level of binding along mutually exclusive areas along MTs, these data suggest that Dcx-T203R doesn't fundamentally disrupt binding.

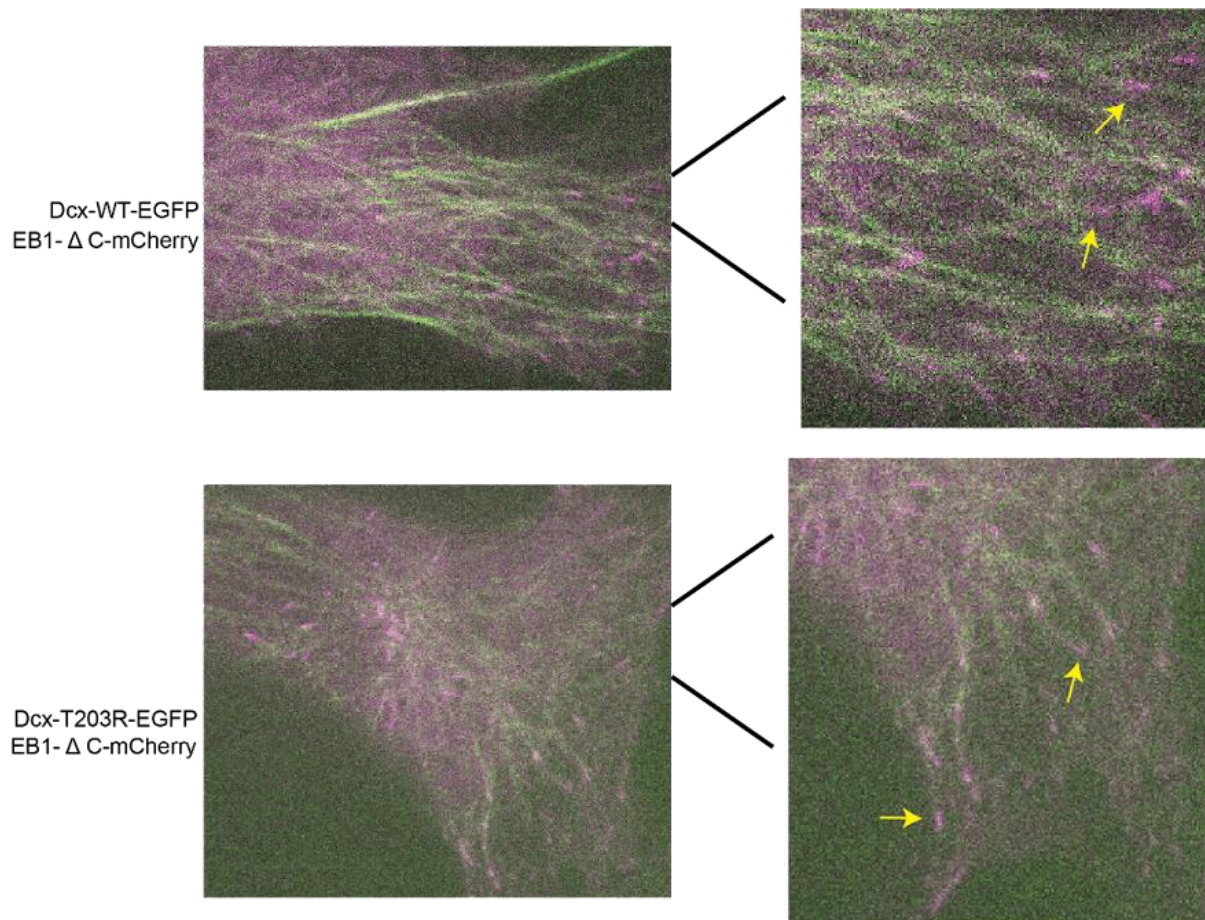


Figure 3.13: Dcx and EB1 Localization in Transfected Fibroblasts

Tail fibroblasts were transfected with either Dcx-WT-EGFP or Dcx-T203R-EGFP (shown in green along MTs) and EB1- Δ – mCherry (shown at the tips of MTs in red). Yellow arrows highlight the mutually exclusive zone of binding for EB1. The localization of Dcx and EB1 does not change between WT and mutant Dcx transfected cells.

Dcx-Microtubule Binding Dynamics vs. Dcx-T203R competitive binding along Microtubules

Previous work has demonstrated that mutations in Dcx may alter binding and stabilization of microtubules (Sapir et al. 2000; Taylor et al. 2000; Schaar, Kinoshita, and McConnell 2004). Our previous experiments also show that Dcx-T203R's binding affinity is lower than that of Dcx-WT, but how would the mutant protein binding along MTs be affected when the WT protein is present within the cell? With this in mind, we wanted to compare the binding affinity to MTs of both Dcx-WT and Dcx-T203R in each other's presence, using a competitive binding assay. We speculated that the Dcx WT protein would have increased binding along MTs when compared to the Dcx-T203R mutant protein, due to the Dcx-T203R amino acid change causing changes in Dcx-MT interactions.

To address this, tail fibroblasts were co-transfected with pLenti6-Dcx-WT-EGFP and pLenti6-Dcx-WT-mCherry plasmids followed by live imaging. Strikingly, under these conditions, we found little to no binding of Dcx-T203R-mCherry, and almost all binding along MTs was with Dcx-WT-EGFP. The mean fluorescence intensity of Dcx-WT-EGFP bound to MTs was nearly 8 times higher than that of Dcx-T203R-mCherry across multiple separate transfections (Fig. 3.14A). Next, to rule out the fluorescent protein as a contributing factor to MT binding, tail fibroblasts were transfected with Dcx-WT-mCherry and Dcx-T203R-EGFP. Once again, the WT protein (in this case fused to mCherry) was almost exclusively binding along MTs with little to no presence of Dcx-T203R-EGFP. The WT protein displayed a mean fluorescence intensity that was almost

six times higher than that of the Dcx-T203R protein (Fig. 3.14B). Lastly, tail fibroblasts were transfected with Dcx-T203R-EGFP and Dcx-T203R-mCherry which would in theory bind at equally low intensity. Indeed, the mean fluorescence intensity between the two was not significantly different and both were bound at relatively low intensities as expected (Fig. 3.14C). Together, this demonstrates that Dcx-T203R binds to MTs at a lower affinity and can be outcompeted by proteins that have a higher binding affinity such as Dcx-WT.

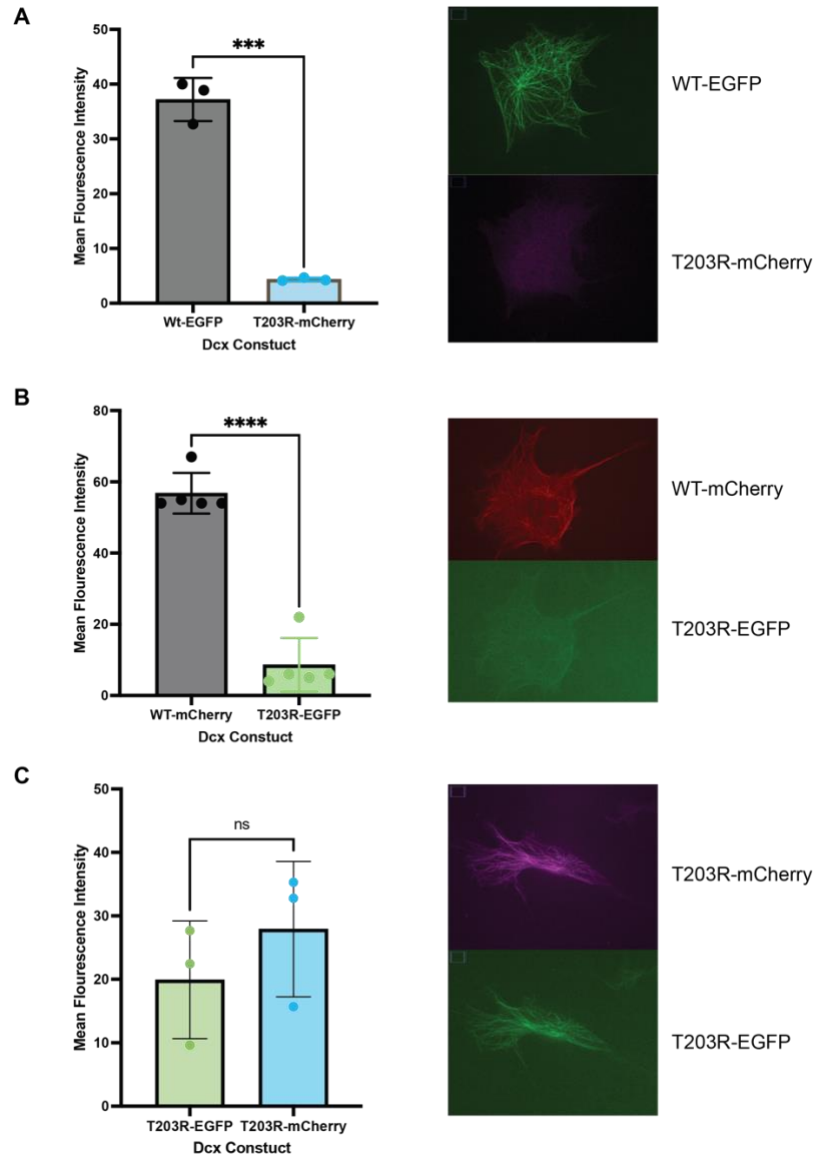


Figure 3.14: Dcx-T203R shows low affinity for microtubules

(A) Tail fibroblasts were transfected with Dcx-WT-EGFP and Dcx-T203R-mCherry constructs and live imaging was performed. Imaging shows little binding of MT by Dcx-T203R-mCherry (right). The mean fluorescence intensity was measured using Fiji and analyzed using an unpaired, two-tailed t-test, $P = 0.0001$ (left). (B) Cells transfected with plasmids that had the fluorescent protein swapped: Dcx-WT-mCherry and Dcx-T203R-EGFP and again showed majority binding along MTs from the WT construct (right). The mean fluorescence intensity was measured using Fiji and analyzed using an unpaired, two-tailed t-test, $P < 0.0001$ (left). (C) Cells were transfected with both mutant constructs: Dcx-T203R-EGFP and Dcx-T203R-mCherry and show equal binding along MTs (C right). The mean fluorescence intensity was measured using Fiji and analyzed using an unpaired, two-tailed t-test, $P = 0.3830$ showing no significance (C left). Each dot on the graphs represents the mean of individual experiments.

Detergent Extractions: Overexpression vs. endogenous expression of mutant Dcx

To further examine the intracellular localization of Dcx, we decided to perform subcellular fractionation experiments. Specifically, we used a detergent extraction method to separate cells into a “pellet” fraction that contains the detergent-insoluble cytoskeleton components and all cytoskeleton-bound proteins, and a “supernatant” fraction which contains lipids and proteins either only loosely-bound or not bound to the cytoskeleton (Sapir et al. 2000; Cohen, Feinstein, and Kimchi 1997). Detergent extractions were performed on tail fibroblasts that were transfected with plasmids containing either Dcx-WT or Dcx-T203R. Cells transfected with Dcx-WT had slightly more Dcx in the pellet fraction than in the supernatant fraction, which was still a substantial portion of all Dcx (Fig. 3.15A). Cells with Dcx-T203R had a much greater proportion of Dcx in the supernatant fraction than in the pellet fraction (Fig. 3.15A).

Next, to assess the distribution of Dcx proteins expressed at endogenous levels from the endogenous *Dcx* locus, detergent extractions were carried out on neurons derived from either WT, both T203R mutant clones (5F and 7C), or Dcx-KO mESCs. Notably, subcellular fractionation has not previously been carried out on neurons expressing a Dcx mutant protein from the endogenous *Dcx* locus. We observed that WT neurons had a majority of Dcx being present in the “pellet” fraction, but still had a small portion of Dcx in the supernatant fraction (Fig. 3.15B). Dcx-T203 expressed in mutant neurons nearly entirely localized to the pellet fraction, similarly to what was observed with WT Dcx, and in stark contrast to the localization of Dcx-T203R observed upon overexpression in fibroblasts (Fig3.15A) and other cell types (Sapir et al. 2000).

This was surprising as it is a significantly different result from what was observed in our transfected cells and what has been previously reported in the literature (Sapir et al. 2000). These results indicate that the cell type and/or levels of expression are critical for physiologic studies of Dcx localization and function.

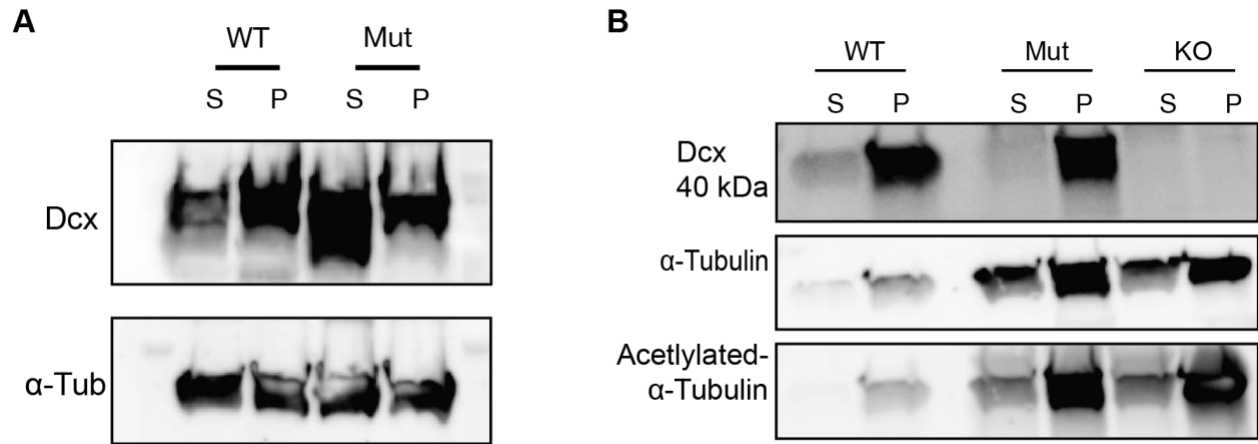


Figure 3.15: Subcellular Fractionation

(A) Subcellular fractionation of tail fibroblasts transfected with either pLenti-Dcx-T203R-mCherry or pLenti-Dcx-WT-mCherry. Detergent extraction shows that cells transfected with the WT construct have slightly more Dcx in the pellet fraction than in the supernatant fraction. In contrast, fibroblasts transfected with the mutant Dcx-T203R construct show a majority of Dcx-T203R in the supernatant fraction. **(B)** Detergent extraction was used to separate the pellet and supernatant fraction of mESC-derived neurons. WT neurons have a small portion of Dcx in the supernatant but most in the pellet fraction. Mutant Dcx-T203R neurons have almost all Dcx localized to the pellet fraction and almost none in the supernatant. Neurons derived from Dcx-KO mESCs were included as negative controls. Loading controls included are α -tubulin, and acetylated- α -tubulin which are more stable tubulin structures.

Chapter 4: Discussion

The results presented in this study demonstrate an in-depth investigation into the introduction and implication of the Dcx-T203R mutation into the mouse endogenous *Dcx* locus. This has allowed us to gain valuable insights into the function of Dcx within neurons and its function as a component of cytoskeletal dynamics and neuronal migration. Until now, most studies of DCX function have focused on complete ablation of the protein, which may leave room for compensation of function by other proteins, or Dcx overexpression, leaving questions about the impact of how specific mutations alter function. By modeling a human disease-causing mutation (DCX-T203R) in mESCs and differentiating them into neurons, we have been able to analyze the phenotypic consequences *in vitro*.

One of the initial concerns was whether the introduction of the disease-causing Dcx-T203R mutation would affect protein expression levels. Our results from western blot analysis in 293T cells expressing either Dcx-WT or T203R-Dcx showed that mutant Dcx-T203R protein is expressed at a similar level to Dcx-WT. This suggests that the mutation itself does not cause protein degradation or significantly impact protein expression.

To rigorously assess the functional implications of the human mutation on protein function, we employed a gene editing approach combining homologous recombination and CRISPR/Cas9 to introduce the Dcx-T203R mutation at the endogenous *Dcx* locus in mESCs, closely mimicking the physiological context. The gene targeted knock-in ES cells were validated using the 'gold-standard' approach (Southern blot) and to further

verify specific insertion of the Dcx-T203R mutation, mutant transcripts were fully validated by cloning and sequencing of the Dcx cDNA transcript.

Our findings in the mESC neuronal differentiation protocol revealed important insights into the impact of Dcx mutation on cell migration, showing a decrease in rate of migration, more so than Dcx-KO neurons. This was surprising as it demonstrates that the Dcx-T203R mutation has a dominant negative effect on the dynamic restructuring of the neuronal cytoskeleton. There were distinct and impactful differences in the dynamic intra-cellular localization of Dcx when comparing the neurons with the introduced endogenous mutation and those that had Dcx-T203R overexpressed (mimicking previous experiments). Further exemplifying the need to accurately model human disease-causing mutations endogenously.

We successfully optimized the neuronal differentiation protocol by removing cyclopamine, an inhibitor of the Hedgehog signaling pathway, and added a transition period for the cells to adjust to the late-differentiation medium which allowed us to robustly derive forebrain neurons from mESCs. With the endogenously targeted neurons derived, we were able to perform a number of in-vitro assays that have led to novel insights. Immunofluorescence microscopy analysis allowed us to comprehensively evaluate the composition of cell types within our cultured samples, including neurons, astrocytes, and oligodendrocytes. Notably, there were some differences in the composition of cell types between Dcx-WT, Dcx-T203R mutant clones, and Dcx-KO cells. This suggests that the mutation did not significantly alter the overall composition of the cultured cells during neuronal differentiation and highlighted

the success of the differentiation protocol. To assess the maturation of cells in culture, we examined the expression of Pax6 and Foxg1 at two different time points during differentiation. There were changes in Foxg1 expression from the early-differentiation stage to the late-differentiation stage, as expected. This indicated proper regional identity of the derived neurons and gave confidence to further analyze the neurons using *in vitro* assays. One striking observation was the presence of Spn-Dcx positive aggregates in the soma and dendrites of Dcx-T203R mutant neurons. These results reinforce the connection between Dcx mutations and Spn-Dcx aggregate formation that has been previously reported (Yap et al. 2016; Tsukada et al. 2003). This suggests that Dcx mutation has a more pronounced effect on aggregate formation and can point to a mechanism that may lead to phenotypes seen in-vivo (Yap et al. 2016). The Dcx-KO neurons also had Spn aggregates that present slightly differently than those found in mutant neurons, both in localization and size of aggregates. Further analysis of what other proteins are aggregating with Spn in the KO neurons is required to determine if the two mechanisms for aggregation are similar.

One possible mechanism for further analysis is the Dcx-T203R interference with a phosphorylation site that is critical for Spn mediated movement of Dcx from MT to the actin filaments found in axon growth cones. Dcx binds with Spn after phosphorylation to initiate the movement and the interference with phosphorylation could cause aggregation of Dcx and obstruction of axon growth cone formation. This would explain the decrease in rate of migration exhibited in mutant neurons. Future experiments can also investigate whether these aggregates form in patient tissue by post-mortem neuropathological analysis.

Our migration assay provided insights into the impact of the specific Dcx-T203R mutation on neuronal migration. Comparing Dcx-WT to Dcx-T203R cells, we observed that WT cells migrated into the scratch at a faster rate, with significantly higher confluence within the scratch area at the end of the 48-hour observation period. Although the data was not shown for both Dcx-T203R neurons, they were both analyzed using the migration assay and had equivalent rates of migration into the scratch. Furthermore, when we included Dcx-KO cells in the analysis, we found that WT cells exhibited superior migration capabilities compared to both mutant and KO cells. Interestingly KO cells had better migration into the scratch than even the mutant cells suggesting a compensatory mechanism for the complete loss of Dcx. Together this suggests that the Dcx-T203R mutation significantly impairs neuronal migration, and has a more severe effect than that of complete Dcx ablation, which underscores the importance of accurately modeling human disease-causing mutations at the endogenous levels.

Our investigation into the intracellular localization and binding dynamics of Dcx-T203R mutant MTs revealed important differences compared to Dcx-WT. Dcx-WT displayed considerably higher levels of fluorescence along MTs compared to Dcx-T203R, indicating a reduced binding affinity of the mutant protein for MTs. Additionally, cells transfected with the Dcx-T203R mutant construct exhibited distinct Dcx-positive aggregates, similar to the aggregates observed in mutant derived (Fig. 3.10). Furthermore, these experiments highlight the disruption caused by Dcx-T203R, leading to aberrant binding dynamics and intracellular localization, causing the formation of aggregates. We also examined whether the mutation affected the mutually exclusive

binding zones of Dcx and EB1 along MTs, but our results indicated that these zones remained conserved in mutant cells. However, the introduction of the Dcx-T203R mutation reduced the intensity of Dcx binding along MTs compared to Dcx-WT, suggesting a potential competitive disadvantage for the mutant protein. Because both DC binding domains in Dcx have a similar structure but different functional properties when binding along MTs, investigation into other patient mutations is needed for information on mechanism of action.

The work presented in this thesis has unveiled new insights into the impact of the Dcx-T203R mutation on various aspects of neuronal biology, including neuronal migration, aggregate formation, and Dcx binding dynamics along MTs. These findings not only enhance our comprehension of the cellular and molecular consequences associated with this disease-causing mutation but also provide a fresh perspective on the potential mechanisms that underlie DCX-related disorders, particularly those that have yet to be explored at the endogenous level. The striking disparities observed in the intracellular localization of Dcx-T203R expressed from the endogenous *Dcx* locus compared to that of mutant Dcx overexpression and complete ablation underscore the necessity for in-depth investigations into the effects of specific disease-causing mutations within their natural cellular context.

Outlook of further studies enabled by the tools and approaches developed during the course of this project

Patient disease-causing missense mutations, which alter the amino acid sequence of DCX, may affect phosphorylation sites or other post-translational modifications or affect protein-protein interactions, thus affecting DCX dynamics and subcellular localization (Schaar, Kinoshita, and McConnell 2004; Tanaka, Serneo, Tseng, et al. 2004; Shmueli et al. 2006). However, such studies can be misleading when performed in the context of *Dcx* overexpression in non-neuronal cells. In future studies, the tools and approaches generated in this project can be used to assess the biochemical properties of *Dcx*-T203R expressed from the endogenous *Dcx* locus, thus eliminating potentially artifactual results associated with overexpression of the mutant protein. Such future studies could include detailed mass spectrometry-based studies of immunoaffinity-purified *Dcx*-T203R protein, using *Dcx*-WT protein and extracts from *Dcx*-KO neurons as controls. Such studies have the potential to comprehensively reveal interacting factors and post-translational modifications and thus shed light on DCX biology.

References

Accogli, Andrea, Nassima Addour-Boudrahem, and Myriam Srour. 2020.

“Neurogenesis, Neuronal Migration, and Axon Guidance.” *Handbook of Clinical Neurology* 173: 25–42.

Ayanlaja, Abiola A., Ye Xiong, Yue Gao, Guangquan Ji, Chuanxi Tang, Zamzam Abdikani Abdullah, and Dianshuai Gao. 2017. “Distinct Features of Doublecortin as a Marker of Neuronal Migration and Its Implications in Cancer Cell Mobility.” *Frontiers in Molecular Neuroscience* 10 (June): 199.

Bai, Jilin, Raddy L. Ramos, James B. Ackman, Ankur M. Thomas, Richard V. Lee, and Joseph J. LoTurco. 2003. “RNAi Reveals Doublecortin Is Required for Radial Migration in Rat Neocortex.” *Nature Neuroscience* 6 (12): 1277–83.

Bechstetd, Susanne, and Gary J. Brouhard. 2012. “Doublecortin Recognizes the 13-Protofilament Microtubule Cooperatively and Tracks Microtubule Ends.” *Developmental Cell* 23 (1): 181–92.

Bedogni, Francesco, Rebecca D. Hodge, Gina E. Elsen, Branden R. Nelson, Ray A. M. Daza, Richard P. Beyer, Theo K. Bammler, John L. R. Rubenstein, and Robert F. Hevner. 2010. “Tbr1 Regulates Regional and Laminar Identity of Postmitotic Neurons in Developing Neocortex.” *Proceedings of the National Academy of Sciences of the United States of America* 107 (29): 13129–34.

Bielas, Stephanie L., Finley F. Serneo, Magdalena Chechlacz, Thomas J. Deerinck, Guy A. Perkins, Patrick B. Allen, Mark H. Ellisman, and Joseph G. Gleeson. 2007. "Spinophilin Facilitates Dephosphorylation of Doublecortin by PP1 to Mediate Microtubule Bundling at the Axonal Wrist." *Cell* 129 (3): 579–91.

Bott, Christopher J., Lloyd P. McMahon, Jason M. Keil, Chan Choo Yap, Kenneth Y. Kwan, and Bettina Winckler. 2020. "Nestin Selectively Facilitates the Phosphorylation of the Lissencephaly-Linked Protein Doublecortin (DCX) by cdk5/p35 to Regulate Growth Cone Morphology and Sema3a Sensitivity in Developing Neurons." *The Journal of Neuroscience: The Official Journal of the Society for Neuroscience* 40 (19): 3720–40.

Cadwell, Cathryn R., Aparna Bhaduri, Mohammed A. Mostajo-Radji, Matthew G. Keefe, and Tomasz J. Nowakowski. 2019. "Development and Arealization of the Cerebral Cortex." *Neuron* 103 (6): 980–1004.

Chang, Amelia N., Zhuoyi Liang, Hai-Qiang Dai, Aimee M. Chapdelaine-Williams, Nick Andrews, Roderick T. Bronson, Bjoern Schwer, and Frederick W. Alt. 2018. "Neural Blastocyst Complementation Enables Mouse Forebrain Organogenesis." *Nature* 563 (7729): 126–30.

Clancy, B., R. B. Darlington, and B. L. Finlay. 2001. "Translating Developmental Time across Mammalian Species." *Neuroscience* 105 (1): 7–17.

Cohen, Dror, Menahem Segal, and Orly Reiner. 2008. "Doublecortin Supports the Development of Dendritic Arbors in Primary Hippocampal Neurons." *Developmental Neuroscience* 30 (1-3): 187–99.

Cohen, O., E. Feinstein, and A. Kimchi. 1997. "DAP-Kinase Is a Ca²⁺/calmodulin-Dependent, Cytoskeletal-Associated Protein Kinase, with Cell Death-Inducing Functions That Depend on Its Catalytic Activity." *The EMBO Journal* 16 (5): 998–1008.

Corbo, Joseph C., Thomas A. Deuel, Jeffrey M. Long, Patricia LaPorte, Elena Tsai, Anthony Wynshaw-Boris, and Christopher A. Walsh. 2002. "Doublecortin Is Required in Mice for Lamination of the Hippocampus but Not the Neocortex." *The Journal of Neuroscience: The Official Journal of the Society for Neuroscience* 22 (17): 7548–57.

Dai, Hai-Qiang, Zhuoyi Liang, Amelia N. Chang, Aimee M. Chapdelaine-Williams, Beatriz Alvarado, Alex A. Pollen, Frederick W. Alt, and Bjoern Schwer. 2020. "Direct Analysis of Brain Phenotypes via Neural Blastocyst Complementation." *Nature Protocols* 15 (10): 3154–81.

Delgado, Ryan N., Denise E. Allen, Matthew G. Keefe, Walter R. Mancia Leon, Ryan S. Ziffra, Elizabeth E. Crouch, Arturo Alvarez-Buylla, and Tomasz J. Nowakowski. 2022. "Individual Human Cortical Progenitors Can Produce Excitatory and Inhibitory Neurons." *Nature*. <https://doi.org/10.1038/s41586-021-04230-7>.

Dema, Alessandro, Rabab A. Charafeddine, Jeffrey van Haren, Shima Rahgozar, Giulia Viola, Kyle A. Jacobs, Matthew L. Kutys, and Torsten Wittmann. 2024. "Doublecortin Reinforces Microtubules to Promote Growth Cone Advance in Soft Environments." *bioRxiv*. <https://doi.org/10.1101/2024.02.28.582626>.

Deuel, Thomas A. S., Judy S. Liu, Joseph C. Corbo, Seung-Yun Yoo, Lucy B. Rorke-Adams, and Christopher A. Walsh. 2006. "Genetic Interactions between Doublecortin

and Doublecortin-like Kinase in Neuronal Migration and Axon Outgrowth.” *Neuron* 49 (1): 41–53.

Dhaliwal, Jagroop, Yanwei Xi, Elodie Bruel-Jungerman, Johanne Germain, Fiona Francis, and Diane C. Lagace. 2015. “Doublecortin (DCX) Is Not Essential for Survival and Differentiation of Newborn Neurons in the Adult Mouse Dentate Gyrus.” *Frontiers in Neuroscience* 9: 494.

Dun, Xin-Peng, Tiago Bandeira de Lima, James Allen, Sara Geraldo, Phillip Gordon-Weeks, and John K. Chilton. 2012. “Drebrin Controls Neuronal Migration through the Formation and Alignment of the Leading Process.” *Molecular and Cellular Neurosciences* 49 (3): 341–50.

Ettinger, Andreas, Jeffrey van Haren, Susana A. Ribeiro, and Torsten Wittmann. 2016. “Doublecortin Is Excluded from Growing Microtubule Ends and Recognizes the GDP-Microtubule Lattice.” *Current Biology: CB* 26 (12): 1549–55.

Fazel Darbandi, Siavash, Sarah E. Robinson Schwartz, Qihao Qi, Rinaldo Catta-Preta, Emily Ling-Lin Pai, Jeffrey D. Mandell, Amanda Everitt, et al. 2018. “Neonatal Tbr1 Dosage Controls Cortical Layer 6 Connectivity.” *Neuron* 100 (4): 831–45.e7.

Francis, F., A. Koulakoff, D. Boucher, P. Chafey, B. Schaar, M. C. Vinet, G. Friocourt, et al. 1999. “Doublecortin Is a Developmentally Regulated, Microtubule-Associated Protein Expressed in Migrating and Differentiating Neurons.” *Neuron* 23 (2): 247–56.

Gaspard, Nicolas, Tristan Bouschet, Adèle Herpoel, Gilles Naeije, Jelle van den Aemele, and Pierre Vanderhaeghen. 2009. "Generation of Cortical Neurons from Mouse Embryonic Stem Cells." *Nature Protocols* 4 (10): 1454–63.

Geschwind, Daniel H., and Pasko Rakic. 2013. "Cortical Evolution: Judge the Brain by Its Cover." *Neuron* 80 (3): 633–47.

Gleeson, J. G., K. M. Allen, J. W. Fox, E. D. Lamperti, S. Berkovic, I. Scheffer, E. C. Cooper, et al. 1998. "Doublecortin, a Brain-Specific Gene Mutated in Human X-Linked Lissencephaly and Double Cortex Syndrome, Encodes a Putative Signaling Protein." *Cell* 92 (1): 63–72.

Gleeson, J. G., P. T. Lin, L. A. Flanagan, and C. A. Walsh. 1999. "Doublecortin Is a Microtubule-Associated Protein and Is Expressed Widely by Migrating Neurons." *Neuron* 23 (2): 257–71.

Gleeson, J. G., S. R. Minnerath, J. W. Fox, K. M. Allen, R. F. Luo, S. E. Hong, M. J. Berg, et al. 1999. "Characterization of Mutations in the Gene Doublecortin in Patients with Double Cortex Syndrome." *Annals of Neurology* 45 (2): 146–53.

Hou, Pei-Shan, Darren Ó. hAilín, Tanja Vogel, and Carina Hanashima. 2020. "Transcription and Beyond: Delineating FOXP1 Function in Cortical Development and Disorders." *Frontiers in Cellular Neuroscience* 14 (February): 35.

Jin, Junghee, Hiromi Suzuki, Syu-Ichi Hirai, Katsuhiko Mikoshiba, and Toshio Ohshima. 2010. "JNK Phosphorylates Ser332 of Doublecortin and Regulates Its Function in

Neurite Extension and Neuronal Migration.” *Developmental Neurobiology* 70 (14): 929–42.

Jin, Kunlin, Xiaomei Wang, Lin Xie, Xiao Ou Mao, and David A. Greenberg. 2010. “Transgenic Ablation of Doublecortin-Expressing Cells Suppresses Adult Neurogenesis and Worsens Stroke Outcome in Mice.” *Proceedings of the National Academy of Sciences of the United States of America* 107 (17): 7993–98.

Kappeler, Caroline, Yoann Saillour, Jean-Pierre Baudoin, Françoise Phan Dinh Tuy, Chantal Alvarez, Christophe Houbron, Patricia Gaspar, et al. 2006. “Branching and Nucleokinesis Defects in Migrating Interneurons Derived from Doublecortin Knockout Mice.” *Human Molecular Genetics* 15 (9): 1387–1400.

Kerjan, Géraldine, Hiroyuki Koizumi, Edward B. Han, Celine M. Dubé, Stevan N. Djakovic, Gentry N. Patrick, Tallie Z. Baram, Stephen F. Heinemann, and Joseph G. Gleeson. 2009. “Mice Lacking Doublecortin and Doublecortin-like Kinase 2 Display Altered Hippocampal Neuronal Maturation and Spontaneous Seizures.” *Proceedings of the National Academy of Sciences of the United States of America* 106 (16): 6766–71.

Kim, Myung Hee, Tomasz Cierpicki, Urszula Derewenda, Daniel Krowarsch, Yuanyi Feng, Yancho Devedjiev, Zbigniew Dauter, et al. 2003. “The DCX-Domain Tandems of Doublecortin and Doublecortin-like Kinase.” *Nature Structural Biology* 10 (5): 324–33.

Koizumi, Hiroyuki, Teruyuki Tanaka, and Joseph G. Gleeson. 2006. “Doublecortin-like Kinase Functions with Doublecortin to Mediate Fiber Tract Decussation and Neuronal Migration.” *Neuron* 49 (1): 55–66.

Kriegstein, Arnold, Stephen Noctor, and Verónica Martínez-Cerdeño. 2006. "Patterns of Neural Stem and Progenitor Cell Division May Underlie Evolutionary Cortical Expansion." *Nature Reviews. Neuroscience* 7 (11): 883–90.

Lim, Lynette, Da Mi, Alfredo Llorca, and Oscar Marín. 2018. "Development and Functional Diversification of Cortical Interneurons." *Neuron* 100 (2): 294–313.

Lin, Hsiu-Chuan, Zhisong He, Sebastian Ebert, Maria Schörnig, Malgorzata Santel, Marina T. Nikolova, Anne Weigert, et al. 2021. "NGN2 Induces Diverse Neuron Types from Human Pluripotency." *Stem Cell Reports* 16 (9): 2118–27.

Liu, Junhua, Mengjie Yang, Mingzhao Su, Bin Liu, Kaixing Zhou, Congli Sun, Ru Ba, et al. 2022. "FOXP1 Sequentially Orchestrates Subtype Specification of Postmitotic Cortical Projection Neurons." *Science Advances* 8 (21): eabh3568.

Lui, Jan H., David V. Hansen, and Arnold R. Kriegstein. 2011. "Development and Evolution of the Human Neocortex." *Cell*. <https://doi.org/10.1016/j.cell.2011.07.005>.

Manka, Szymon W., and Carolyn A. Moores. 2020. "Pseudo-Repeats in Doublecortin Make Distinct Mechanistic Contributions to Microtubule Regulation." *EMBO Reports* 21 (12): e51534.

Mao, Xiang, and Shasha Zhao. 2020. "Neuronal Differentiation from Mouse Embryonic Stem Cells In Vitro." *Journal of Visualized Experiments: JoVE*, no. 160 (June). <https://doi.org/10.3791/61190>.

Martinez-Cerdeno, V. 2006. "The Role of Intermediate Progenitor Cells in the Evolutionary Expansion of the Cerebral Cortex." *Cerebral Cortex* 16 (Supplement 1): i152–61.

Matsumoto, N., R. J. Leventer, J. A. Kuc, S. K. Mewborn, L. L. Dudleycek, M. B. Ramocki, D. T. Pilz, et al. 2001. "Mutation Analysis of the DCX Gene and Genotype/phenotype Correlation in Subcortical Band Heterotopia." *European Journal of Human Genetics: EJHG* 9 (1): 5–12.

Merz, Katharina, and D. Chichung Lie. 2013. "Evidence That Doublecortin Is Dispensable for the Development of Adult Born Neurons in Mice." *PloS One* 8 (5): e62693.

Moffat, Jeffrey J., Minhan Ka, Eui-Man Jung, and Woo-Yang Kim. 2015. "Genes and Brain Malformations Associated with Abnormal Neuron Positioning." *Molecular Brain* 8 (1): 72.

Moores, Carolyn A., Mylène Perderiset, Fiona Francis, Jamel Chelly, Anne Houdusse, and Ronald A. Milligan. 2004. "Mechanism of Microtubule Stabilization by Doublecortin." *Molecular Cell* 14 (6): 833–39.

Moslehi, Maryam, Dominic C. H. Ng, and Marie A. Bogoyevitch. 2017. "Dynamic Microtubule Association of Doublecortin X (DCX) Is Regulated by Its C-Terminus." *Scientific Reports* 7 (1): 5245.

Noctor, Stephen C., Verónica Martínez-Cerdeño, Lidija Ivic, and Arnold R. Kriegstein. 2004. "Cortical Neurons Arise in Symmetric and Asymmetric Division Zones and Migrate through Specific Phases." *Nature Neuroscience* 7 (2): 136–44.

Nosten-Bertrand, Marika, Caroline Kappeler, Céline Dinocourt, Cécile Denis, Johanne Germain, Françoise Phan Dinh Tuy, Soraya Verstraeten, et al. 2008. "Epilepsy in *Dcx* Knockout Mice Associated with Discrete Lamination Defects and Enhanced Excitability in the Hippocampus." *PloS One* 3 (6): e2473.

Nowakowski, Tomasz J., Alex A. Pollen, Carmen Sandoval-Espinosa, and Arnold R. Kriegstein. 2016. "Transformation of the Radial Glia Scaffold Demarcates Two Stages of Human Cerebral Cortex Development." *Neuron* 91 (6): 1219–27.

Ohshima, T., J. M. Ward, C. G. Huh, G. Longenecker, Veeranna, H. C. Pant, R. O. Brady, L. J. Martin, and A. B. Kulkarni. 1996. "Targeted Disruption of the Cyclin-Dependent Kinase 5 Gene Results in Abnormal Corticogenesis, Neuronal Pathology and Perinatal Death." *Proceedings of the National Academy of Sciences of the United States of America* 93 (20): 11173–78.

Pramparo, Tiziano, Yong Ha Youn, Jessica Yingling, Shinji Hirotsune, and Anthony Wynshaw-Boris. 2010. "Novel Embryonic Neuronal Migration and Proliferation Defects in *Dcx* Mutant Mice Are Exacerbated by *Lis1* Reduction." *The Journal of Neuroscience: The Official Journal of the Society for Neuroscience* 30 (8): 3002–12.

Rafiei, Atefeh, Sofía Cruz Tetlalmatzi, Claire H. Edrington, Linda Lee, D. Alex Crowder, Daniel J. Saltzberg, Andrej Sali, Gary Brouhard, and David C. Schriemer. 2022.

“Doublecortin Engages the Microtubule Lattice through a Cooperative Binding Mode Involving Its C-Terminal Domain.” *eLife* 11 (April). <https://doi.org/10.7554/eLife.66975>.

Ramos, Raddy L., Jilin Bai, and Joseph J. LoTurco. 2006. “Heterotopia Formation in Rat but Not Mouse Neocortex after RNA Interference Knockdown of DCX.” *Cerebral Cortex* 16 (9): 1323–31.

Reiner, Orly, Frédéric M. Coquelle, Bastian Peter, Talia Levy, Anna Kaplan, Tamar Sapir, Irit Orr, Naama Barkai, Gregor Eichele, and Sven Bergmann. 2006. “The Evolving Doublecortin (DCX) Superfamily.” *BMC Genomics* 7 (January): 188.

Reiner, Orly, Amos Gdalyahu, Indraneel Ghosh, Talia Levy, Sivan Sapoznik, Ronit Nir, and Tamar Sapir. 2004. “DCXs Phosphorylation by Not Just aNother Kinase (JNK).” *Cell Cycle* 3 (6): 745–49.

Rice, Sarah E. 2001. *A Structural Change in the Neck Region of Kinesin Motors Drives Unidirectional Motility*. University of California, San Francisco.

Sansom, Stephen N., Dean S. Griffiths, Andrea Faedo, Dirk-Jan Kleinjan, Youlin Ruan, James Smith, Veronica van Heyningen, John L. Rubenstein, and Frederick J. Livesey. 2009. “The Level of the Transcription Factor Pax6 Is Essential for Controlling the Balance between Neural Stem Cell Self-Renewal and Neurogenesis.” *PLoS Genetics* 5 (6): e1000511.

Sapir, T., D. Horesh, M. Caspi, R. Atlas, H. A. Burgess, S. G. Wolf, F. Francis, et al. 2000. "Doublecortin Mutations Cluster in Evolutionarily Conserved Functional Domains." *Human Molecular Genetics* 9 (5): 703–12.

Schaar, Bruce T., Kazuhisa Kinoshita, and Susan K. McConnell. 2004. "Doublecortin Microtubule Affinity Is Regulated by a Balance of Kinase and Phosphatase Activity at the Leading Edge of Migrating Neurons." *Neuron* 41 (2): 203–13.

Shahsavani, M., R. J. Pronk, R. Falk, M. Lam, M. Moslem, S. B. Linker, J. Salma, et al. 2018. "An in Vitro Model of Lissencephaly: Expanding the Role of DCX during Neurogenesis." *Molecular Psychiatry* 23 (7): 1674–84.

Shmueli, Anat, Amos Gdalyahu, Sivan Sapoznik, Tamar Sapir, Miki Tsukada, and Orly Reiner. 2006. "Site-Specific Dephosphorylation of Doublecortin (DCX) by Protein Phosphatase 1 (PP1)." *Molecular and Cellular Neurosciences* 32 (1): 15–26.

Stepien, Barbara K., Ronald Naumann, Anja Holtz, Jussi Helppi, Wieland B. Huttner, and Samir Vaid. 2020. "Lengthening Neurogenic Period during Neocortical Development Causes a Hallmark of Neocortex Expansion." *Current Biology: CB* 30 (21): 4227–37.e5.

Tanaka, Teruyuki, Finley F. Serneo, Christine Higgins, Michael J. Gambello, Anthony Wynshaw-Boris, and Joseph G. Gleeson. 2004. "Lis1 and Doublecortin Function with Dynein to Mediate Coupling of the Nucleus to the Centrosome in Neuronal Migration." *The Journal of Cell Biology* 165 (5): 709–21.

Tanaka, Teruyuki, Finley F. Serneo, Huang Chun Tseng, Ashok B. Kulkarni, Li Huei Tsai, and Joseph G. Gleeson. 2004. "Cdk5 Phosphorylation of Doublecortin ser297 Regulates Its Effect on Neuronal Migration." *Neuron* 41 (2): 215–27.

Taylor, K. R., A. K. Holzer, J. F. Bazan, C. A. Walsh, and J. G. Gleeson. 2000. "Patient Mutations in Doublecortin Define a Repeated Tubulin-Binding Domain." *The Journal of Biological Chemistry* 275 (44): 34442–50.

Thoma, Eva C., Erhard Wischmeyer, Nils Offen, Katja Maurus, Anna-Leena Sirén, Manfred Schartl, and Toni U. Wagner. 2012. "Ectopic Expression of Neurogenin 2 Alone Is Sufficient to Induce Differentiation of Embryonic Stem Cells into Mature Neurons." *PloS One* 7 (6): e38651.

Tsukada, Miki, Alexander Prokscha, and Gregor Eichele. 2006. "Neurabin II Mediates Doublecortin-Dephosphorylation on Actin Filaments." *Biochemical and Biophysical Research Communications* 343 (3): 839–47.

Tsukada, Miki, Alexander Prokscha, Judit Oldekamp, and Gregor Eichele. 2003. "Identification of Neurabin II as a Novel Doublecortin Interacting Protein." *Mechanisms of Development* 120 (9): 1033–43.

Tsukada, Miki, Alexander Prokscha, Ernst Ungewickell, and Gregor Eichele. 2005. "Doublecortin Association with Actin Filaments Is Regulated by Neurabin II." *The Journal of Biological Chemistry* 280 (12): 11361–68.

Vallee, Richard B., John C. Williams, Dileep Varma, and Lora E. Barnhart. 2004.

“Dynein: An Ancient Motor Protein Involved in Multiple Modes of Transport.” *Journal of Neurobiology* 58 (2): 189–200.

Vanderhaeghen, Pierre. 2012. “Chapter 10 - Generation of Cortical Neurons from Pluripotent Stem Cells.” In *Progress in Brain Research*, edited by Stephen B. Dunnett and Anders Björklund, 201:183–95. Elsevier.

Yap, Chan Choo, Laura Digilio, Kamil Kruczek, Matylda Roszkowska, Xiao-Qin Fu, Judy S. Liu, and Bettina Winckler. 2018. “A Dominant Dendrite Phenotype Caused by the Disease-Associated G253D Mutation in Doublecortin (DCX) Is Not due to Its Endocytosis Defect.” *The Journal of Biological Chemistry* 293 (49): 18890–902.

Yap, Chan Choo, Laura Digilio, Lloyd McMahon, Matylda Roszkowska, Christopher J. Bott, Kamil Kruczek, and Bettina Winckler. 2016. “Different Doublecortin (DCX) Patient Alleles Show Distinct Phenotypes in Cultured Neurons: EVIDENCE FOR DIVERGENT LOSS-OF-FUNCTION AND ‘OFF-PATHWAY’ CELLULAR MECHANISMS.” *The Journal of Biological Chemistry* 291 (52): 26613–26.

Ye, Liu, Beibei Liu, Jingling Huang, Xiaolin Zhao, Yuan Wang, Yungen Xu, and Shuping Wang. 2023. “DCLK1 and Its Oncogenic Functions: A Promising Therapeutic Target for Cancers.” *Life Sciences* 336 (November): 122294.

Yoshiura, K., Y. Noda, A. Kinoshita, and N. Niikawa. 2000. “Colocalization of Doublecortin with the Microtubules: An Ex Vivo Colocalization Study of Mutant Doublecortin.” *Journal of Neurobiology* 43 (2): 132–39.

Zhang, Xiaoqing, Cindy T. Huang, Jing Chen, Matthew T. Pankratz, Jiajie Xi, Jin Li, Ying Yang, et al. 2010. "Pax6 Is a Human Neuroectoderm Cell Fate Determinant." *Cell Stem Cell* 7 (1): 90–100.

Zheng, Y., M. L. Wong, B. Alberts, and T. Mitchison. 1995. "Nucleation of Microtubule Assembly by a Gamma-Tubulin-Containing Ring Complex." *Nature* 378 (6557): 578–83.
583.

Publishing Agreement

It is the policy of the University to encourage open access and broad distribution of all theses, dissertations, and manuscripts. The Graduate Division will facilitate the distribution of UCSF theses, dissertations, and manuscripts to the UCSF Library for open access and distribution. UCSF will make such theses, dissertations, and manuscripts accessible to the public and will take reasonable steps to preserve these works in perpetuity.

I hereby grant the non-exclusive, perpetual right to The Regents of the University of California to reproduce, publicly display, distribute, preserve, and publish copies of my thesis, dissertation, or manuscript in any form or media, now existing or later derived, including access online for teaching, research, and public service purposes.

DocuSigned by:

Beatriz Alvarado

D211065259B342A...

Author Signature

3/18/2024

Date